DAHLGREN DIVISION
NAVAL SURFACE WARFARE CENTER
Dahlgren, Virginia 22448-5100

NSWCDD/TR-95/206

USING GPS TO DETERMINE AN ASTRONOMIC-GEODETIC TRANSFORMATION FOR A PRECISE AZIMUTH REFERENCE (PAR)

BY BRUCE R. HERMANN JAMES CUNNINGHAM

STRATEGIC AND SPACE SYSTEMS DEPARTMENT

DECEMBER 1995

REPORT DOCUMENTATION PAGE

Form Approved
OMB No. 0704-0188

1. AGENCY USE ONLY (Leave blank)	2. REPORT DATE	3. REPORT TYPE AND DATES COVERED
	December 1995	

4. TITLE AND SUBTITLE
Using GPS to Determine an Astronomic-Geodetic Transformation for a Precise Azimuth Reference (PAR)

5. FUNDING NUMBERS

6. AUTHOR(s)

B. R. Hermann, J. Cunningham

7. PERFORMING ORGANIZATION NAME(S) AND ADDRESS(ES)

Commander
Naval Surface Warfare Center
Dahlgren Division (Code K12)
17320 Dahlgren Road
Dahlgren, VA 22448-5100

8. PERFORMING ORGANIZATION REPORT NUMBER

NSWCDD/TR-95/206

9. SPONSORING/MONITORING AGENCY NAME(S) AND ADDRESS(ES)

10. SPONSORING/MONITORING AGENCY REPORT NUMBER

11. SUPPLEMENTARY NOTES

12a. DISTRIBUTION/AVAILABILITY STATEMENT

Approved for public release; distribution is unlimited.

12b. DISTRIBUTION CODE

13. ABSTRACT (Maximum 200 words)

A technique is presented to generate a transformation between the astronomic and geodetic reference frames. The transformation is based on knowing the orientation of a plane in both reference frames. The plane's astronomic orientation is assumed to be known. The geodetic orientation is determined using Global Positioning System (GPS) kinematic relative positioning. For the problem addressed in the report, the plane is a window used to make astronomic observations at Holloman Air Force Base, New Mexico. A precise azimuth reference at an accuracy approaching 0.1 arcsec is derived using observations of the star Polaris. Because the window is inaccessible and cannot be instrumented with GPS antennas, an indirect measurement technique is explored. GPS multipath signals reflected off the window are evaluated as a means whereby the orientation of the window may be determined. The viability of this method is untested. Results from a static positioning test are presented to demonstrate the technique of determining the plane's geodetic orientation. Orientation consistency on the order of 1 arcsec is obtained.

14. SUBJECT TERMS

precise azimuth, GPS, kinematic relative positioning, geodetic coordinates, astronomic coordinates, radar range equation

15. NUMBER OF PAGES

16. PRICE CODE

17. SECURITY CLASSIFICATION OF REPORTS	18. SECURITY CLASSIFICATION OF THIS PAGE	19. SECURITY CLASSIFICATION OF ABSTRACT	20. LIMITATION OF ABSTRACT
UNCLASSIFIED	UNCLASSIFIED	UNCLASSIFIED	UL

FOREWORD

Since the 1960s, a precise azimuth reference (PAR) has been maintained at Holloman Air Force Base, New Mexico. Currently, this azimuth reference is maintained by the Defense Mapping Agency (DMA) at an accuracy approaching 0.1 arcsec. In the early 1980s a requirement was established to significantly improve this reference to support accuracies approaching 0.01 arcsec. Current Global Positioning System (GPS) kinematic relative positioning surveys reach subcentimeter accuracies over baselines varying from hundreds of meters to hundreds of kilometers. At 100 km, a 5-mm perpendicular error is equivalent to 0.01 arcsec.

Astronomic measurements with the new Geodetic Astrolabe, along with radiometry to measure and correct for relative tropospheric refraction, suggest that accuracies to better than 0.1 arcsec are possible. Together, these Astronomic techniques coupled with GPS indicate that a GPS/stellar reference of 0.05 arcsec is within reason.

The current 0.1 arcsec reference is optically determined. To use it with GPS determined azimuths, the two results need to be placed in a common coordinate system. GPS results are found in the World Geodetic System 1984 (WGS 84); consequently, azimuths determined this way are geodetic azimuths. Stellar observations give azimuths in astronomic coordinates. The relationships between these two systems can be found if the difference between the local gravity vector and the normal to the ellipsoid are known. Alternately, a reference surface whose position and orientation are known in both systems would suffice. The accuracy with which the GPS can determine the orientation of a plane in space is investigated. This work was funded by DMA under the direction of Mr. Ben Roth and Mr. Dennis Bredthauer and was performed in the Space and Geodesy Branch, Space and Surface Systems Division, Strategic and Space Systems Department.

The authors would like to thank Mr. Roth and Mr. Bredthauer for their support of this project. The authors would also like to thank Dr. Alan G. Evans for his helpful comments.

This report has been reviewed by Dr. Jeffrey N. Blanton, Head, Space and Geodesy Branch and Mr. James L. Sloop, Head, Space and Surface Systems Division.

Approved by:

D.B. COLBY, Head
Strategic and Space Systems Department

CONTENTS

ILLUSTRATIONS

TABLES

1.0 INTRODUCTION

A precise azimuth reference (PAR) at Holloman Air Force Base, New Mexico, is maintained by the Defense Mapping Agency (DMA) at an accuracy approaching 0.1 arc second. Currently at Holloman, azimuth observations of the star Polaris with an autocollimating theodolite are used to derive the reference. Theodolite observations determine astronomic azimuth while many field applications require geodetic azimuth. The transformation between the laboratory's astronomic azimuth and geodetic azimuth used in the field is the main topic of this report. A brief discussion of possible techniques to improve the accuracy of the PAR is presented in Appendix A.

The autocollimating theodolite points through a laboratory window. Using the window's position in both the astronomic and geodetic reference frames, a transformation between the two frames can be generated. Assuming the window's astronomic position is known, finding its geodetic position becomes the primary problem. High precision World Geodetic System 1984 (WGS 84) positions can be determined using Global Positioning System (GPS) measurements. Unfortunately, the window is inaccessible and cannot be instrumented with GPS antennas. The desire to exploit GPS accuracy has led to the suggestion that the GPS signal reflections (multipath) from the window be used to define its position (Reference 1). In a general way, employing the signal multipath is similar to kinematic GPS relative positioning.

Kinematic GPS relative positioning involves determining the position of a moving receiver with respect to a fixed one (Reference 2). Both carrier phases and pseudoranges are collected from a minimum of four satellites. It has been demonstrated that the baseline vector between the fixed and remote sites can be determined to the millimeter level (References 3 and 4). One advantage of kinematic over static relative positioning is that a baseline vector is determined at every observation time. This is an important property because, although the laboratory window is stationary, the reflection point will move with time because of changing geometry. The moving reflection point is analogous to a moving receiver. Kinematic positioning therefore allows any motion around the nominal reflection point to be observed. This can be useful as a diagnostic because the incident signals come from different directions and their reflection points will be different unless the physical size of the reflective area is small.

Assumptions will be made in the development of the astronomic to geodetic transformation. Foremost, it has not been demonstrated in the laboratory that tracking a multipath signal is possible, although theoretically the concept has been introduced (Reference 5). Aside from the difficulties of gaining lock for a multipath signal, it is assumed that the window can be represented mathematically as a plane.

2.0 REFERENCE FRAMES

The Earth's form is often approximated by an ellipsoid whose shorter axis is the axis of revolution. Small deviations between the actual form of the Earth and the ellipsoid of revolution are the source of the differences between the astronomic and geodetic reference frames. Astronomic coordinates are based on astronomic observations made with level instruments. Because they are directly based on observations, they are also called natural coordinates. Geodetic coordinates are based on the ellipsoid of revolution. Both astronomic and geodetic coordinates (latitude and longitude) are referred to the Conventional Terrestrial System (CTS). The CTS has its origin at the center of the Earth; the X-axis is towards the mean astronomic Greenwich meridian; the Z-axis is towards the Conventional Terrestrial Pole; the Y-axis is perpendicular to both and forms a right-handed coordinate system.

Leveling an astronomic instrument makes its vertical parallel the direction of the gravity vector at the station. The direction of the gravity vector is sometimes called the plumb line. Astronomic latitude (Figure 2-1) is the angle measured in the astronomic meridian plane between the instrument's plumb line and the equatorial plane. It is positive from the equator northward, and negative to the south. The equatorial plane is defined perpendicular to the Earth's rotation axis. Instantaneous and mean astronomic latitudes are defined by using, respectively, the instantaneous and mean equatorial planes. Astronomic longitude is the equatorial angle from the prime meridian to the astronomic meridian plane containing the parallel to the rotation axis and the plumb line. It is positive to the east. An instantaneous or mean rotation axis is used to define, respectively, an instantaneous or mean astronomic longitude. The instantaneous rotation axis is located with respect to the mean rotation axis (the Z-axis of the CTS) by the elements of polar motion. Astronomic height is the orthometric height of the station. Orthometric height is measured along the curved plumb line from the geoid.

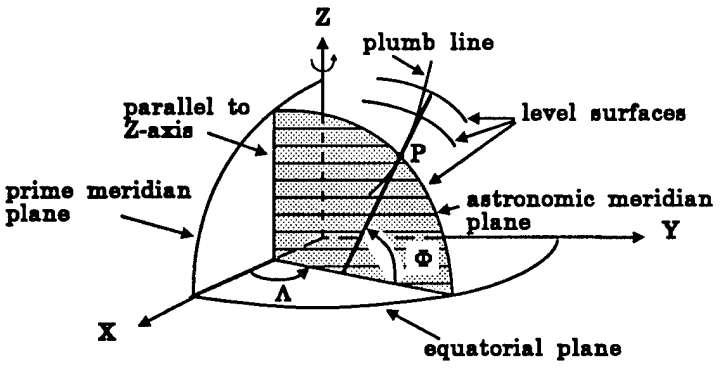

FIGURE 2-1. ASTRONOMIC LATITUDE (Φ) AND LONGITUDE (Λ) OF STATION P

Geodetic latitude (Figure 2-2) is the angle measured in the meridian plane between the ellipsoid's equatorial plane and the line that is normal to the ellipsoid and also passes through the station. It is positive northward and negative southward. Geodetic longitude is the angle measured in the equatorial plane between the prime meridian and the meridian passing through the station. It is positive to the east. Geodetic height is the straight line distance from the ellipsoid measured along the ellipsoidal normal.

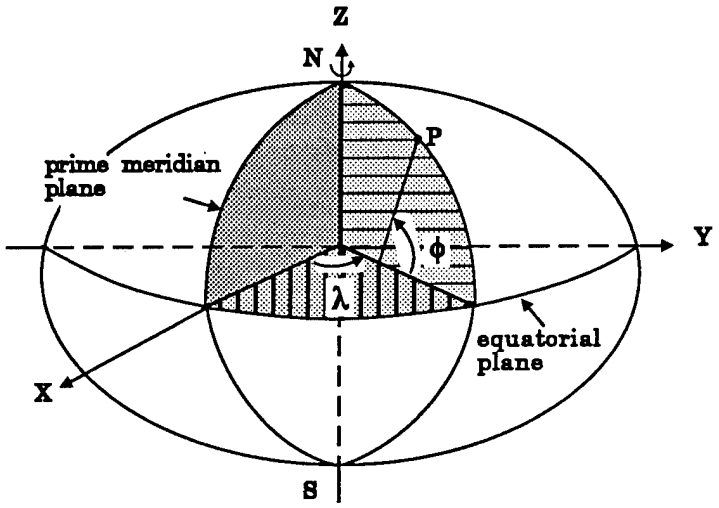

FIGURE 2-2. GEODETIC LATITUDE (ϕ) AND LONGITUDE (λ) OF STATION P

The conversion of astronomic latitude and longitude to their geodetic counterparts involves the deflection of the vertical (Reference 6). Equation (2-1) shows the relationship between astronomic and geodetic latitude, and Equation (2-2) shows the relationship for astronomic and geodetic longitude.

$$\phi = \Phi - \xi \tag{2-1}$$

$$\lambda = \Lambda - \eta \sec(\phi) \tag{2-2}$$

where ϕ is the geodetic latitude
Φ is astronomic latitude
ξ is the north-south component of deflection of the vertical
λ is geodetic longitude
Λ is astronomic longitude
η is the east-west component of deflection of the vertical

The astronomic latitude and longitude and the components of the deflection of the vertical given in these equations are referenced to the station location and not the geoid. Equation (2-3) gives an approximate relationship between geodetic height and astronomic height. Figure (2-3) is a sketch showing the geometric relationships of these quantities.

$$h = H + N \tag{2-3}$$

where h is the geodetic height
H is the astronomic height
N is the geoidal undulation

Using this approximation should result in geodetic and astronomic coordinates consistent to within less than 0.01 arcsec.

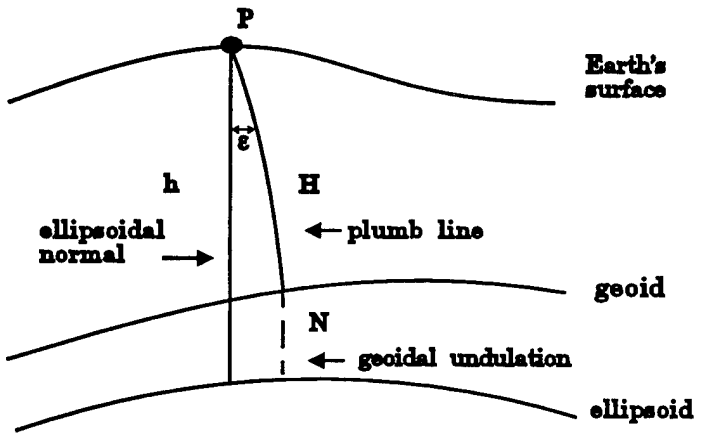

FIGURE 2-3. GEODETIC HEIGHT (h), ASTRONOMIC HEIGHT (H), GEOIDAL UNDULATION (N), AND TOTAL DEFLECTION OF THE VERTICAL (ε) OF STATION P

The WGS 84 consists of an ellipsoid definition, a reference frame, and gravity field and geoid models (References 7,8, and 9). The definition of the WGS 84 ellipsoid has recently been reviewed. Among the four defining WGS 84 parameters, only the geocentric gravitational constant, GM, was altered. The International Earth Rotation Service (IERS) GM value was adopted for high-accuracy Department of Defense applications such as precise orbit determination (Reference 10). The WGS 84 reference frame (i.e., a set of station coordinates) was refined using GPS data from worldwide networks of tracking stations (Reference 11). The refined WGS 84 reference frame and the IERS Terrestrial Reference Frame 1991 (ITRF91) are estimated to be coincident to within 10 cm (Reference 11). Currently a joint project involving DMA and the National Aeronautics and Space Administration is underway to improve the WGS 84 gravity field and geoid models.

3.0 PROPOSED TECHNIQUE

The fundamental problem is to determine the WGS 84 position of a plane target by using GPS signal reflections. Figure 3-1 shows a schematic of the problem's geometry. Pseudorange and phase data are collected at the absolute reference antenna (labeled *A* in the figure). At this antenna multipath is a noise source to be eliminated. The directional antenna (labeled *B*) points to the plane target (labeled *T*). The directional antenna collects both pseudorange and phase data reflected from the target. The vector $\mathbf{v}_{AB}$ connecting the two antennas transfers the absolute position to the directional antenna. This vector might be surveyed independently or simultaneously depending on the properties of the directional antenna. The vector $\mathbf{v}_{BT}$ from the directional antenna to the nominal reflection point on the static target is constant. At any time the actual reflection point depends on the relative position of the satellites and the target. The satellite-target geometry changes because of satellite motion and Earth rotation over the span of observation. The reflection points should describe a continuous path around the nominal target. Kinematic relative positioning solutions can be made to follow the path of the reflections. To initiate the solution, an On-The-Fly (OTF) ambiguity resolution technique is necessary in order to resolve the integer cycle ambiguities.

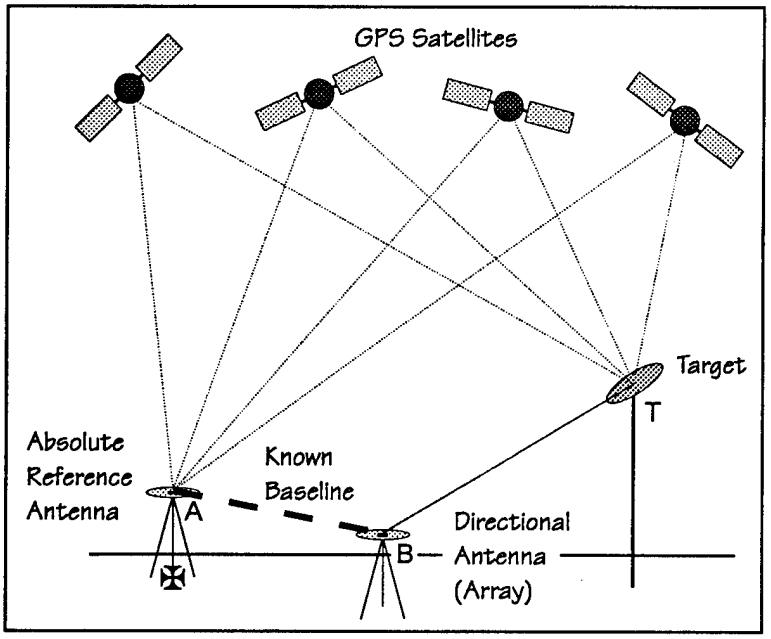

FIGURE 3-1. SATELLITE SIGNALS ARE REFLECTED FROM TARGET AT T TO RECEIVING ANTENNA AT B

Using the positions of three or more reflection points, the orientation of the WGS 84 best-fitting plane can be determined. The transformation between the geodetic and astronomic frames can be determined using the orientation of the plane in the two frames.

4.0 OBSERVATION EQUATIONS

A review of the GPS observation equations is presented to investigate what modes of operation may be best suited for PAR applications. Kinematic relative positioning using phase observations are the most precise and are recommended. Dual frequency solutions to remove the ionospheric effects are not needed over short baselines. Since the ionospheric correction adds noise to the observation, single frequency solutions are probably the best choice. Double differencing between the receivers and the satellites removes both satellite and local clock offsets. Single differences between satellites produce lower noise observations, but long-term drift due to receiver clock or equivalent sources are judged to be a serious problem. Therefore double differenced solutions are recommended.

4.1 GPS OBSERVATION MODEL

Obtaining the best results over baselines of 1 km and longer kinematic relative positioning requires the use of both pseudorange and phase observations at L_1 and L_2 frequencies. Single frequency observations can be used when the separation distances are small and the differential range bias from the ionosphere can be neglected. A model that describes the pseudorange observation was presented by Braasch (Reference 12). The notation will be modified for the purposes here, but the general form will be retained. For each parameter, a dependance upon satellite will be expressed as a superscript j or k, and a dependance upon receiver (and antenna) will be expressed by a subscript m or n. The transmission frequency is denoted by the subscript f, which may be either a 1 or a 2, and the time of the observation is denoted by the subscript i. Absence of a dependance is represented by a dot. Figure 4-1 shows some vectors used in the observation equations derived below.

Braasch's observation equation includes the following terms: the true geometric range ${r^j}_{m.i}$ between receiver antenna i and satellite j, the receiver time offset $\tau_{m.i}$, the satellite time offset ${\tau^j}_{..i}$, propagation effects due to the troposphere ${T^j}_{m.i}$ and the ionosphere ${I^j}_{mfi} = (\lambda^2_f/c)\,{K^j}_{m.i}$, the User Range Error *URE*, multipath error d_{MP}, receiver satellite channel delay d_{HW}, receiver measurement bias errors d_{MEAS}, receiver noise, and the deliberately introduced effects of Selective Availability ${SA^j}_{..i}$. In the following development, the User Range Error, multipath error, receiver channel delay, bias errors, and noise will be omitted, but a term to account for relativistic effects ${\gamma^j}_{m.i}$ will be added. The ionospheric constant ${K^j}_{m.i}$ is related to the columnar electron content along the line of sight (Reference 13). The pseudorange observation ${\rho^j}_{mli}$ for satellite j, receiver m, frequency 1, and observation i, with meters as units, is written in Equation (4-1).

$$\rho^j_{m1i} = r^j_{m.i} + \gamma^j_{m.i} + c\,(\tau_{m.i} - \tau^j_{..i}) + T^j_{m.i} + \frac{\lambda_1^2}{c} K^j_{m.i} + SA^j_{..i} \qquad (4\text{-}1)$$

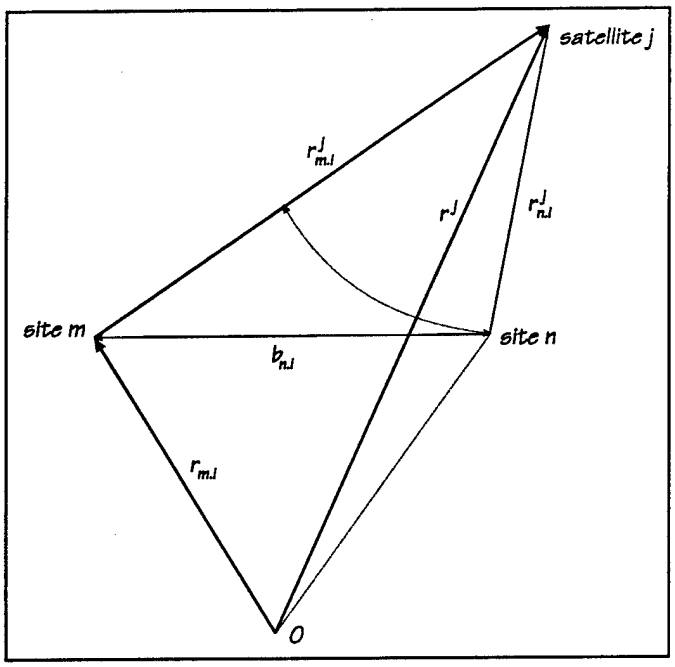

FIGURE 4-1. SOME VECTORS USED IN OBSERVATION EQUATIONS

A similar expression can be used for the phase observation if an integer cycle ambiguity term N^j_{m10} is added. It represents the number of full cycle counts recorded by the receiver on a particular channel and is arbitrary. Since the integer cycle ambiguity is part of the phase observation, it will be included on the left-hand side in Equation (4-2). When N^j_{m10} is correctly known, the sum of the phase ϕ^j_{m1i} (cycles) plus the integer N^j_{m10} (cycles) represents the observed range $R^j_{m.i}$ (meters) divided by the wavelength (meters). The sum has units of cycles. The wavelength λ_1 is needed in Equation (4-2) to change these cycles back to meters. Note that the ionospheric refraction in Equation (4-2) has the opposite sign that it had in Equation (4-1) (Reference 14).

$$\lambda_1(\phi^j_{m1i} + N^j_{m1.}) = r^j_{m.i} + \gamma^j_{m.i} + c(\tau_{m.i} - \tau^j_{..i}) + T^j_{m.i} - \frac{\lambda_1^2}{c} K^j_{m.i} + SA^j_{..i} \qquad (4\text{-}2)$$

The geometric range $r^j_{m.i}$ is the magnitude of the vector to the satellite, in the WGS 84 coordinate system, minus the vector to the receiver antenna, as shown in Equation (4-3). The satellite coordinates as a function of time are available from the satellite ephemerides, while the receiver antenna coordinates are to be found. With relative positioning between multiple sites, it is assumed that at least one of those sites is known or can be found in an absolute sense in the WGS 84 reference frame. The kinematic relative positioning technique locates one site with respect to another precisely, even when all sites are in motion with respect to the earth, but is not intended for the absolute determination of position.

$$r^j_{m.i} = r^j_{..i} - r_{m.i} = (x^j_{..i} - x_{m.i})\hat{x} + (y^j_{..i} - y_{m.i})\hat{y} + (z^j_{..i} - z_{m.i})\hat{z} \qquad (4\text{-}3)$$

4.2 SMOOTHING PSEUDORANGE WITH PHASE

As shown in Equation (4-2), the phase observations have an unknown range bias $N^j_{m1.}$ that is site-, satellite-, and frequency-dependent. Therefore the phase observations cannot be used to obtain a navigation solution in the same manner as the pseudoranges, because there is an added unknown range bias introduced by each satellite. This is unfortunate because the noise associated with a single frequency pseudorange observation is about an order of magnitude greater than the noise on the equivalent phase observation. Multipath is also less pronounced with phase (References 15 and 16). For these reasons, when pseudoranges are needed but an instantaneous real time navigation solution is not the primary objective, it is advantageous to use the phases to smooth the pseudoranges.

4.2.1 Single Frequency Observations

In order to smooth the pseudoranges, continuous uninterrupted phase observations from all satellites are required over the entire period of interest. The idea is to reduce the random error on the initial pseudorange observation by averaging. In effect, the pseudoranges at any time t_i become the sum of the initial averaged pseudorange plus the difference between the phase observation at t_i and the initial phase at t_0. The ionospheric effect remains and is expressed by the terms containing $K^j_{m.i}$ in the equations that follow.

By differencing between Equations (4-1) and (4-2) all the terms on the right-hand side are removed except for the ionospheric component. This result for t_i is shown in Equation (4-4).

$$\rho^j_{m1i} - \lambda_1 (\phi^j_{m1i} + N^j_{m1.}) = 2 \frac{\lambda_1^2}{c} K^j_{m.i} \qquad (4\text{-}4)$$

By differencing in time two equations like (4-4), the unknown integer $N^j_{m1.}$ can be removed. Equation (4-5) shows the difference between observations at t_i and t_0.

$$\rho^j_{m1i} - \rho^j_{m10} = \lambda_1 (\phi^j_{m1i} - \phi^j_{m10}) + 2 \frac{\lambda_1^2}{c} (K^j_{m.i} - K^j_{m.0}) \qquad (4\text{-}5)$$

Equation (4-5) can be rearranged so that all the terms relating to t_0 are on the left-hand side. They are expressed in terms of the pseudorange and the ionospheric term at each succeeding time, plus the phase differences as shown in Equation (4-6).

$$\rho^j_{m10} - 2 \frac{\lambda_1^2}{c} K^j_{m.0} = \rho^j_{m1i} - 2 \frac{\lambda_1^2}{c} K^j_{m.i} - \lambda_1 (\phi^j_{m1i} - \phi^j_{m10}) \qquad (4\text{-}6)$$

The average pseudorange, denoted by the overbar in Equation (4-7), is evaluated at t_0 by summing Equation (4-6) over all κ observation times.

The average pseudorange, denoted by the overbar in Equation (4-7), is evaluated at t_0 by summing Equation (4-6) over all κ observation times.

$$\overline{\rho^j_{m10} - 2\frac{\lambda_1^2}{c}K^j_{m.0}} = \frac{1}{\kappa + 1}\sum_{i=0}^{\kappa}\left[\rho^j_{m1i} - 2\frac{\lambda_1^2}{c}K^j_{m.i} - \lambda_1(\phi^j_{m1i} - \phi^j_{m10})\right] \tag{4-7}$$

Now the pseudorange at each time t_i can be reconstructed by rearranging Equation (4-6) and inserting the average value for the pseudorange at t_0 from Equation (4-7). The result, Equation (4-8), is the smoothed pseudorange observation equation for L_1. If L_2 observations are available, the same procedure can be applied to them. In cases where two-frequency data is available, it may be useful to remove the ionospheric term. The procedure for removing the ionospheric effect is discussed in section 4.2.3.

$$\rho^j_{m1i} - 2\frac{\lambda_1^2}{c}K^j_{m.i} = \overline{\rho^j_{m10} - 2\frac{\lambda_1^2}{c}K^j_{m.0}} + \lambda_1(\phi^j_{m1i} - \phi^j_{m10}) \tag{4-8}$$

4.2.2 Time Differences

Single frequency time differences can be used to remove the differential ionospheric effects that accummulate over time. A second benefit of time differences is that it provides a way to detect cycle slips. A cycle slip is a phenomenon that occurs when the receiver mistracks the satellite signal without losing lock and adds or subtracts multiple integers (or half integers, depending upon the receiver design) to the phase observation. Since each integer cycle slip adds or subtracts a wavelength of range between the receiver antenna and the satellite, it can lead to an erroneous position solution.

Time differences can be computed to perform the tasks outlined above. The pseudorange time difference, derived from Equation (4-1), is shown in Equation (4-9) and the phase time difference, derived from Equation (4-2), is shown in Equation (4-10). Assuming that there are no cycle slips between epochs t_0 and t_i, the integer cycle term $N^j_{m1.}$ subtracts out in Equation (4-10).

$$\begin{aligned}\rho^j_{m1i} - \rho^j_{m10} = {} & \frac{\lambda_1^2}{c}(K^j_{m.i} - K^j_{m.0}) + \\ & (r^j_{m.} - r^j_{m.0}) + (\gamma^j_{m.i} - \gamma^j_{m.0}) + c(\tau_{m.i} - \tau_{m.0}) - c(\tau^j_{..i} - \tau^j_{..0}) + \\ & (T^j_{m.i} - T^j_{m.0}) + (SA^{\,j}_{..i} - SA^{\,j}_{..0})\end{aligned} \tag{4-9}$$

$$\lambda_1(\phi^j_{m1i} - \phi^j_{m10}) = -\frac{\lambda_1^2}{c}(K^j_{m.i} - K^j_{m.0}) + (r^j_{m.i} - r^j_{m.0}) + (\gamma^j_{m.i} - \gamma^j_{m.0}) + c(\tau_{m.i} - \tau_{m.0}) - c(\tau^j_{..i} - \tau^j_{..0}) + (T^j_{m.i} - T^j_{m.0}) + (SA^{\ j}_{..i} - SA^{\ j}_{..0}) \quad (4\text{-}10)$$

Since only single frequency observations are being considered, the two frequency method described in section 4.2.3 cannot be used to eliminate the ionospheric term K^j_{m1i} from the observations. When Equation (4-10) is subtracted from (4-9), all the terms on the right-hand side of the equal sign are removed except for the ionospheric terms. The resulting estimate of the ionospheric range difference in the interval $(t_i - t_0)$ is shown in Equation (4-11) and can be substituted into either (4-9) or (4-10) to remove the differential ionospheric term. Since pseudoranges are included in (4-11), this scheme will add noise to the phase observations in (4-10).

$$\frac{\lambda_1^2}{c}(K^j_{m.i} - K^j_{m.0}) = \frac{1}{2}[(\rho^j_{m1i} - \rho^j_{m10}) - \lambda_1(\phi^j_{m1i} - \phi^j_{m10})] \quad (4\text{-}11)$$

Cycle slips can be identified by comparing the differentially corrected versions of (4-9) and (4-10). With the ionospheric term removed, the remainder of the right hand side of the two equations are the same. Therefore the left-hand sides must measure the same range difference. If the difference between the phase equation and the pseudorange equation departs from zero after a period of time, a cycle slip might have occurred in the phase.

4.2.3 Dual Frequency Observations

The ionospheric term can be computed from (4-10) if two-frequency phase data are available. Once the ionospheric effect is removed, the pseudoranges can be smoothed by the phases to reduce the random noise in the same way as was done previously for the single frequency case. First, form the differences as in Equation (4-10) for both L_1 and L_2. Then difference the two time differences. All the terms on the right in (4-10) are independent of frequency except the ionospheric term. The result of the difference is written as Equation (4-12).

$$\lambda_1(\phi^j_{m1i} - \phi^j_{m10}) - \lambda_2(\phi^j_{m2i} - \phi^j_{m20}) = \left(\frac{\lambda_2^2 - \lambda_1^2}{c}\right)(K^j_{m.i} - K^j_{m.0}) \quad (4\text{-}12)$$

Each of the ionospheric terms is modeled by a frequency-independent parameter $K^j_{m.i}$, which is proportional to the ionospheric electron content along the line of sight, between each receiver antenna and each satellite. A solution for the constants is possible in terms of the phase observations and their respective wavelengths, as shown in Equation (4-13).

$$K^{j}_{m.t} - K^{j}_{m.0} = c\left(\frac{\lambda_1(\phi^{j}_{m1t} - \phi^{j}_{m10}) - \lambda_2(\phi^{j}_{m2t} - \phi^{j}_{m20})}{\lambda_2^2 - \lambda_1^2}\right) \tag{4-13}$$

If Equation (4-13) is multiplied by $2(\lambda^2_1/c)$ and added to both sides of (4-10), a time-differenced observation, Equation (4-14), is created that has the same right-hand side as the pseudorange time difference Equation (4-9). Equation (4-14) has the same functional properties as the pseudorange but with the low-noise properties of phase (Reference 14).

$$\begin{aligned}\lambda_1(\phi^{j}_{m1t} - \phi^{j}_{m10}) + 2\lambda_1^2\left(\frac{\lambda_1(\phi^{j}_{m1t} - \phi^{j}_{m10}) - \lambda_2(\phi^{j}_{m2t} - \phi^{j}_{m20})}{\lambda_2^2 - \lambda_1^2}\right) = \\ \frac{\lambda_1^2}{c}(K^{j}_{m.t} - K^{j}_{m.0}) + (r^{j}_{m.t} - r^{j}_{m.0}) + (\gamma^{j}_{m.t} - \gamma^{j}_{m.0}) + \\ c(\tau_{m.t} - \tau_{m.0}) - c(\tau^{j}_{..t} - \tau^{j}_{..0}) + (T^{j}_{m.t} - T^{j}_{m.0}) + (SA^{j}_{..t} - SA^{j}_{..0})\end{aligned} \tag{4-14}$$

Since the right-hand side of Equation (4-14) is the same as the right-hand side of (4-9), the left-hand sides of those two equations must be equal. Exploiting this, the pseudorange at t_i can be rewritten in terms of the two-frequency phase observations and the pseudorange at t_0, as in Equation (4-15). A similar expression can be written for L_2 if desired.

$$\rho^{j}_{m1t} = \rho^{j}_{m10} + \lambda_1(\phi^{j}_{m1t} - \phi^{j}_{m10}) + 2\lambda_1^2\left(\frac{\lambda_1(\phi^{j}_{m1t} - \phi^{j}_{m10}) - \lambda_2(\phi^{j}_{m2t} - \phi^{j}_{m20})}{\lambda_2^2 - \lambda_1^2}\right) \tag{4-15}$$

Equation (4-15) can be rearranged to find an average value for ρ^{j}_{m10} as was done for the single frequency case. This average can then be substituted into Equation (4-15), and the smoothed, ionospherically corrected pseudoranges computed from the phases. Equation (4-16) is used to compute this average pseudorange at t_0. All of the smoothing performed in this section can be performed with data from a single receiver. In the next section, multiple receivers and satellites are considered.

$$\overline{\rho^{j}_{m10}} = \frac{1}{\kappa + 1}\sum_{t=0}^{\kappa}\left\{\rho^{j}_{m1t} - \lambda_1(\phi^{j}_{m1t} - \phi^{j}_{m10}) - 2\lambda_1^2\left(\frac{\lambda_1(\phi^{j}_{m1t} - \phi^{j}_{m10}) - \lambda_2(\phi^{j}_{m2t} - \phi^{j}_{m20})}{\lambda_2^2 - \lambda_1^2}\right)\right\} \tag{4-16}$$

4.3 SINGLE DIFFERENCE BETWEEN RECEIVERS

If two sites collect pseudorange and phase data from the same set of satellites simultaneously, the observations can be differenced to remove some effects that are common to both. When performing these differences, the absolute motion of the sites with respect to the satellites, or the relative motion between the two sites (if any) is not important. What is important is that the velocity and acceleration of the receiver antennas with respect to the satellites be such that the GPS receivers retain continuous track of the signals and do not introduce time tag errors (due to tracking loop delays) when reporting the observations. Also, the receiver's clocks should not be widely divergent in either time or frequency offsets (Reference 17).

When pseudorange observation equations in the form of Equation (4-1) are differenced between receivers m and n, Equation (4-17) results. Because the satellite-dependent time offset $\tau^{j}_{..i}$ and Selective Availability $SA^{j}_{..i}$ are common to both observations, they are effectively removed by the difference.

$$\rho^{j}_{mJi} - \rho^{j}_{nJi} = \frac{\lambda_J^2}{c}(K^{j}_{m.i} - K^{j}_{n.i}) + (r^{j}_{m.i} - r^{j}_{n.i}) + (\gamma^{j}_{m.i} - \gamma^{j}_{n.i}) + c(\tau_{m.i} - \tau_{n.i}) + (T^{j}_{m.i} - T^{j}_{n.i}) \tag{4-17}$$

Equation (4-18) shows the result of differencing the phase observations, taken from Equation (4-2), between the two receivers m and n. As in the pseudorange, the satellite-dependent terms drop out.

$$\lambda_J(\phi^{j}_{mJi} - \phi^{j}_{nJi} + N^{j}_{mJ.} - N^{j}_{nJ.}) = -\frac{\lambda_J^2}{c}(K^{j}_{m.i} - K^{j}_{n.i}) + (r^{j}_{m.i} - r^{j}_{n.i}) + (\gamma^{j}_{m.i} - \gamma^{j}_{n.i}) + c(\tau_{m.i} - \tau_{n.i}) + (T^{j}_{m.i} - T^{j}_{n.i}) \tag{4-18}$$

4.4 DOUBLE DIFFERENCE BETWEEN RECEIVERS AND SATELLITES

Equations (4-17) and (4-18) can be formed for each of the satellites that are common between the observation sites. A second difference can be computed between satellites; this produces a double difference in which the site-specific terms, such as local clock biases, are removed. What remains is relativity, propagation effects due to the ionosphere and troposphere, the geometric range, and in the case of the phase observation, the unknown integer phase counts. Equation (4-19) is the double differenced form of the pseudorange observations, and Equation (4-20) is the double differenced form of the phase observation.

$$(\rho^{j}_{mJi} - \rho^{j}_{nJi}) - (\rho^{k}_{mJi} - \rho^{k}_{nJi}) =$$

$$\frac{\lambda_1^2}{c}\left[(K^{j}_{m.i} - K^{j}_{n.i}) - (K^{k}_{m.i} - K^{k}_{n.i})\right] + (r^{j}_{m.i} - r^{j}_{n.i}) - (r^{k}_{m.i} - r^{k}_{n.i}) + \tag{4-19}$$

$$(\gamma^{j}_{m.i} - \gamma^{j}_{n.i}) - (\gamma^{k}_{m.i} - \gamma^{k}_{n.i}) + (T^{j}_{m.i} - T^{j}_{n.i}) - (T^{k}_{m.i} - T^{k}_{n.i})$$

$$\lambda_1\left[(\phi^{j}_{mJi} - \phi^{j}_{nJi} + N^{j}_{mJ.} - N^{j}_{nJ.}) - (\phi^{k}_{mJi} - \phi^{k}_{nJi} + N^{k}_{mJ.} - N^{k}_{nJ.})\right] =$$

$$-\frac{\lambda_1^2}{c}\left[(K^{j}_{m.i} - K^{j}_{n.i}) - (K^{k}_{m.i} - K^{k}_{n.i})\right] + (r^{j}_{m.i} - r^{j}_{n.i}) - (r^{k}_{m.i} - r^{k}_{n.i}) + \tag{4-20}$$

$$(\gamma^{j}_{m.i} - \gamma^{j}_{n.i}) - (\gamma^{k}_{m.i} - \gamma^{k}_{n.i}) + (T^{j}_{m.i} - T^{j}_{n.i}) - (T^{k}_{m.i} - T^{k}_{n.i})$$

Note that for short baselines where the paths to the satellite from both receivers are approximately the same, the ionospheric terms in Equations (4-19) and (4-20) contribute little to the observed range and can be ignored. For longer baselines the ionospheric terms may need to be considered. As was done previously in Equation (4-12), the two-frequency observations can be differenced to eliminate all but the ionospheric contribution. This is shown for the phase in Equation (4-21).

$$\lambda_1\left[(\phi^{j}_{mJi} - \phi^{j}_{nJi} + N^{j}_{mJ.} - N^{j}_{nJ.}) - (\phi^{k}_{mJi} - \phi^{k}_{nJi} + N^{k}_{mJ.} - N^{k}_{nJ.})\right] -$$

$$\lambda_2\left[(\phi^{j}_{m2i} - \phi^{j}_{n2i} + N^{j}_{m2.} - N^{j}_{n2.}) - (\phi^{k}_{m2i} - \phi^{k}_{n2i} + N^{k}_{m2.} - N^{k}_{n2.})\right] = \tag{4-21}$$

$$\left(\frac{\lambda_2^2 - \lambda_1^2}{c}\right)\left[(K^{j}_{m.i} - K^{j}_{n.i}) - (K^{k}_{m.i} - K^{k}_{n.i})\right]$$

It can be seen that Equation (4-21) may be solved for the *K*'s and then substituted back into Equation (4-20). The *K*'s are written explicitly in terms of the phase observations and integer ambiguities in Equation (4-22).

$$\left[(K^j_{m.i} - K^j_{n.i}) - (K^k_{m.i} - K^k_{n.i})\right] =$$

$$c\lambda_1 \frac{\left[(\phi^j_{m1i} - \phi^j_{n1i} + N^j_{m1.} - N^j_{n1.}) - (\phi^k_{m1i} - \phi^k_{n1i} + N^k_{m1.} - N^k_{n1.})\right]}{\lambda_2^2 - \lambda_1^2} -$$

$$c\lambda_2 \frac{\left[(\phi^j_{m2i} - \phi^j_{n2i} + N^j_{m2.} - N^j_{n2.}) - (\phi^k_{m2i} - \phi^k_{n2i} + N^k_{m2.} - N^k_{n2.})\right]}{\lambda_2^2 - \lambda_1^2} \qquad (4\text{-}22)$$

When Equation (4-22) is substituted into Equation (4-20), the ionospheric effect is removed and the ranges plus the effects of relativity and tropospheric refraction are expressed in terms of the two-frequency phase observations and the integers. The ionospherically corrected double differenced observation equation is given in Equation (4-23).

$$\frac{\lambda_1\lambda_2^2}{\lambda_2^2 - \lambda_1^2}\left[(\phi^j_{m1i} - \phi^j_{n1i} + N^j_{m1.} - N^j_{n1.}) - (\phi^k_{m1i} - \phi^k_{n1i} + N^k_{m1.} - N^k_{n1.})\right] -$$

$$\frac{\lambda_1^2\lambda_2}{\lambda_2^2 - \lambda_1^2}\left[(\phi^j_{m2i} - \phi^j_{n2i} + N^j_{m2.} - N^j_{n2.}) - (\phi^k_{m2i} - \phi^k_{n2i} + N^k_{m2.} - N^k_{n2.})\right] = \qquad (4\text{-}23)$$

$$(r^j_{m.i} - r^j_{n.i}) - (r^k_{m.i} - r^k_{n.i}) + (\gamma^j_{m.i} - \gamma^j_{n.i}) - (\gamma^k_{m.i} - \gamma^k_{n.i}) + (T^j_{m.i} - T^j_{n.i}) - (T^k_{m.i} - T^k_{n.i})$$

A comparison of Equation (4-23) with Equation (4-20) illustrates the advantage of using single frequency observations when possible. The noise in the L_1 observations expressed in the first line of Equation (4-23) are multiplied by a factor $\frac{\lambda_2^2}{\lambda_2^2 - \lambda_1^2}$, which is 2.55 compared to unity for the same observations in Equation (4-20). In addition, the L_2 observations, which do not appear in Equation (4-20), are multiplied by a factor of $\frac{\lambda_1^2}{\lambda_2^2 - \lambda_1^2}$, or 1.55 times the wavelength. Therefore for lowest double differenced noise over short baselines, where the differential ionospheric effects between sites can be neglected, single frequency observations should be used. A discussion of the ionospheric tradeoffs is given by Clynch and Coco (Reference 18).

For the particular case where the best relative positioning noise performance is desired over short static baselines, the single difference alternative should be considered. Equation (4-18) shows that the observation noise should be about 0.7 of the doubly differenced case because only one satellite is considered per observation, rather than two. Besides the ionospheric and tropospheric refraction and relativity effects, there remains the difference between the local frequency standards. If the two

receivers are locked to a single high-performance frequency standard and temperature effects are controlled, this difference could be kept small enough to ignore. However, Gourevitch (Reference 19) cautions that the Ashtech Z-12 receiver is optimized for double differencing and that differential phase drifts between receivers can and do occur. This is probably true of any manufacturers. These drifts look like clock drifts and will appear when other modes of processing that do not eliminate the local clock are used. Therefore it seems prudent to employ double differencing kinematic techniques to avoid common mode problems due to receiver hardware environmental dependencies.

4.5 SOLUTION PROCEDURE

For the purposes of this discussion of kinematic relative positioning, assume that two frequency pseudorange and phase data are available from two sites and four or more satellites over a period of time. The time interval between observations should be as short as possible consistent with the correlation time between solutions due to receiver bandwidth and the dynamics of the sites, if any. In general, no constraints need be placed upon the motion of either site; both may be moving with respect to the WGS 84 geodetic coordinate system, though that will not be desirable for PAR. It has been demonstrated that the kinematic relative positioning procedure allows precise relative positions to be reliably computed between two (or more) sites over distances up to about 30 km.

4.5.1 The Reference Site

To begin, one needs to know the location of the reference site. The reference may be assigned to any site, but it is usually the one that is centrally located and well defined. It can be at rest or in motion, but if there is a site at rest, it should be selected as the reference. When possible, it should occupy a preexisting bench mark and thus tie the positions of the other sites to an absolute reference. If in motion, then the other sites will be positioned with respect to it and provide three-dimensional information about the relative vectors joining them as a function of time. Whether the reference is in motion or not, an estimate of its absolute position is required so that the partial derivatives can be computed. If *a priori* information is not available, the conventional navigation solution computed with pseudoranges should be adequate in most cases. Pseudoranges smoothed with phases should be used to minimize the observation noise.

In order to smooth the pseudoranges, Equation (4-8) can be used. The pseudoranges from all succeeding times t_i are shifted by the phase observations to t_0 and averaged over the κ observation epochs. The navigation solution at t_0 can then be computed with the averaged pseudoranges. If two-frequency pseudoranges are available, another equation like Equation (4-8) can be written for L_2, and the two used together to compute the ionospheric correction. Alternatively, the equations developed in section 4.2.3 can be used. Then the solution for the position and local time offset of the reference site can be computed if four or more satellite observations are available.

4.5.2 Secondary Sites

With the reference position known at each time epoch to within the errors allowed by the navigation solution or site survey, an estimate of the other site's position with respect to the reference is needed. If the position of the site is known at t_0, no initial estimate of the position is needed. Otherwise, a navigation solution similar to the one described for the reference site can be computed for the initial position.

With the baselines approximately known, a procedure to establish the unknown integer cycle ambiguities can then be employed to precisely define the baseline vectors at each time epoch. The reference site, if in motion, is not a factor in the accuracy with which the relative solutions may be obtained.

4.6 OTF INITIALIZATION

The reference site is either at a fixed position, or its position as function of time must be found from a navigation solution using the smoothed pseudoranges obtained from Equation (4-16). The integer cycle ambiguities can be established without requiring that both sites be stationary for a period of time (Reference 20). Assume that an OTF integer ambiguity resolution technique has provided an estimate of the position of the secondary site with respect to the reference at each observation epoch. Once found, these integers can be used to continue to compute the kinematic relative position of all sites relative to the reference. Equation (4-20) and its equivalent for L_2 may be used, or alternatively, the two-frequency observation Equation (4-23) for sites that are separated by several kilometers may be used.

5.0 OBSERVATION EQUATIONS FOR PAR

For the PAR application, a plane is defined in space by computing the vector from a given reference antenna to three or more points that lie in a plane. If just three points are used, the plane is defined by those points. If more than three points are used, then the plane must be some best fit to all points as described later in this report. Figure 5-1 illustrates the case where the plane target is defined by three patch antennas. The antenna at point A is the absolute reference. It operates in the ordinary sense by collecting pseudorange and phase data via the direct signal from the satellites. The antennas at T_1, T_2, and T_3 also receive the direct signals from the satellites. The baselines from point A to each of the target points T_1, T_2, and T_3 are found from kinematic relative positioning. However, in this application the target is inaccessible and cannot be instrumented with patch antennas.

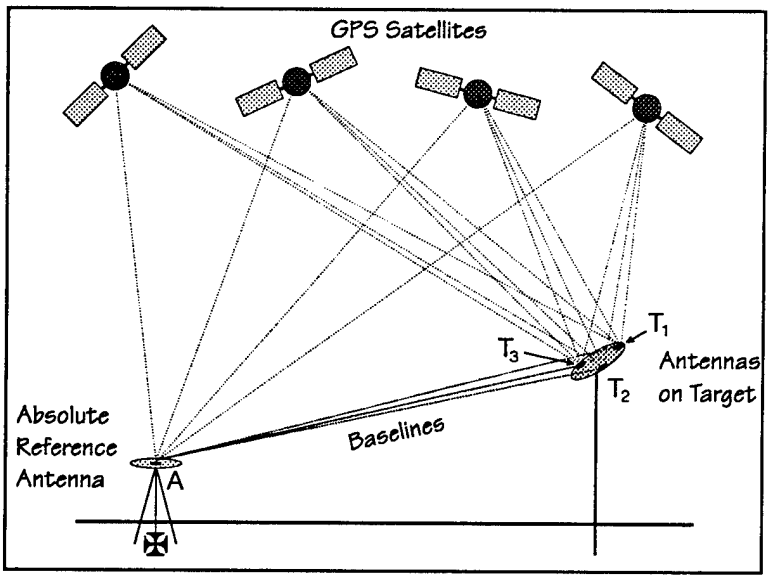

FIGURE 5-1. BASELINE VECTORS FROM A TO TARGET DETERMINE PLANE T_1, T_2, T_3

In Figure 5-2 the situation is modified by the addition of a directional antenna array represented by the antenna at point B. In this case there are no antennas at the target; rather, the signals are assumed to be reflected from the target and received at B. The direct signals from the satellites to B must be attenuated so that they do not swamp the desired indirect signals from T. For this reason, no direct rays are shown to reach the antenna at B. The reference antenna at A continues to operate as before. Now the kinematic relative positioning is between antennas A and B, where B receives the indirect signals from the target. The distance between the antenna at B and any point on the target is constant and the kinematic relative positioning is between antennas A and B, where B receives the indirect signals from the target. The distance between the antenna at B and any point on the target is constant

and satellite-independent. This extra propagation distance acts just like an antenna cable delay or local clock offset. The effect is the same as if the antenna at B were physically located at a point on the target. Therefore the data analysis proceeds just as it would in the situation illustrated in Figure 5-1.

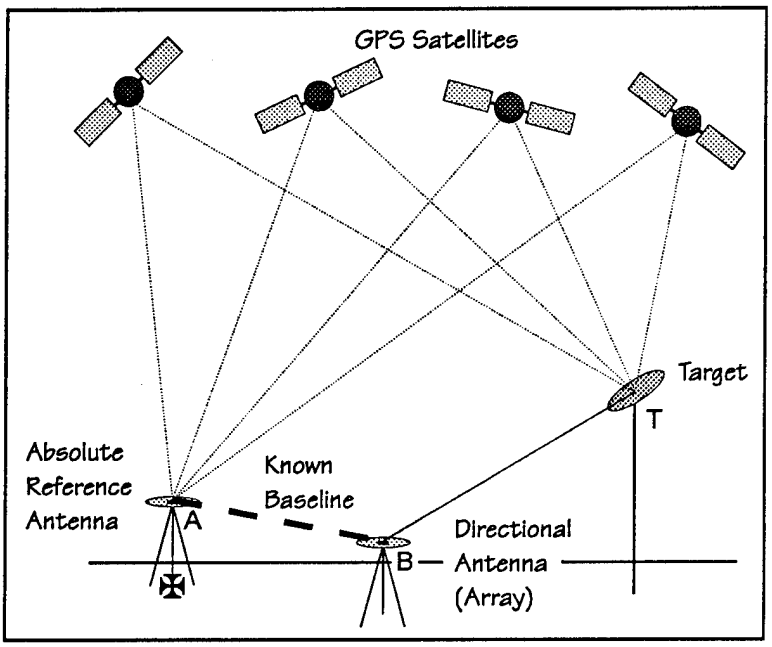

FIGURE 5-2. BASELINE VECTORS FROM A TO B DETERMINE TARGET PLANE

This can be demonstrated from the pseudorange observation equation. The pseudorange, or phase observation, is written in terms of the magnitude of the vector difference between the satellite position j and the site location m (the range), plus other terms, as in Equation (5-1).

$$\rho^{j}_{m.i} = r^{j}_{m.i} + \gamma^{j}_{m.i} + c\,(\tau_{m.i} - \tau^{j}_{..i}) + T^{j}_{m.i} + \frac{\lambda_1^2}{c} K^{j}_{m.i} + SA^{j}_{..i} \qquad (5\text{-}1)$$

The vector from the site m to the satellite j can be expressed in terms of the vector to the satellite minus the vector to the site, as in Equation (5-2).

$$r^{j}_{m.i} = r^{j}_{..i} - r_{m.i} \qquad (5\text{-}2)$$

In the indirect case, the site subscript m represents the incidence of the indirect signals at T. No direct signals from the satellites are received at B, only the indirect signals. Therefore the geometric range is the sum of the range from satellite j to the target T and from T to antenna B, as written in Equation (5-3). The paired vertical bars indicate *magnitude of.*

$$indirect\ range = r^{j}_{T,i} + r_{BT,i} = \left| r^{j}_{\cdot,i} - r_{T,i} \right| + \left| r_{T,i} - r_{B,i} \right| \qquad (5\text{-}3)$$

This expression takes the place of $r^{j}_{m,i}$ in Equation (5-1). Since the second term in Equation (5-3) is independent of satellite j, and the points representing the target and antenna B are fixed points, the range is constant and can be lumped with the $c\,\tau_{m,i}$ term that is also satellite-independent.

6.0 PAR TRANSFORMATION SOLUTION

Using the GPS techniques outlined above, the positions of points on the laboratory window at Holloman can be determined in the WGS 84. The window is assumed to be a flat surface and is modeled as a plane. When a sufficient number of GPS observations are available, a least squares solution for the plane's orientation is made. Given the astronomic coordinates of the plane and the WGS 84 orientation, a transformation that relates the astronomic and geodetic frames is found.

6.1 EQUATION OF A PLANE IN THE WGS 84

The most direct method of defining the general equation of a plane uses three noncollinear points. Three such points in the WGS 84 are defined as Q with Cartesian coordinates at x_q, y_q, z_q, R at x_r, y_r, z_r, and S at x_s, y_s, z_s. The vector **N** is defined normal to the WGS 84 plane on which Q, R and S exist. The point P represents any point on that plane. By definition, the dot product of the vector from Q to P and vector **N** is zero:

$$\overline{(QP)} \cdot N = 0 \tag{6-1}$$

Defining the vector **N** as the cross product of two vectors in the WGS 84 plane:

$$N = \overline{QR} \times \overline{QS} \tag{6-2}$$

then the dot product in Equation (6-1) becomes:

$$\overline{(QP)} \cdot (\overline{QR} \times \overline{QS}) = 0 \tag{6-3}$$

After expanding Equation (6-3), the closed form expression of a WGS 84 plane is:

$$\begin{aligned} &(x - x_q)\,[(y_r - y_q)\,(z_s - z_q) - (y_s - y_q)\,(z_r - z_q)] \\ &+ (y - y_q)\,[(x_s - x_q)\,(z_r - z_q) - (x_r - x_q)\,(z_s - z_q)] \\ &+ (z - z_q)\,[(x_r - x_q)\,(y_s - y_q) - (x_s - x_q)\,(y_r - y_q)] = 0 \end{aligned} \tag{6-4}$$

6.2 DETERMINATION OF A PLANE IN SPACE

As described above, three points define a plane, but in the case of the PAR, there will be multiple determinations of points that must lie on one plane. These points may be referenced to a single external reference point R as illustrated in Figure 6-1. The vectors V_{Ri} represent individual determinations of a vector to each of several points that must lie on the plane. A least squares solution can perform the desired synthesis and combine all the point solutions into an estimate of the plane that best fits all observations.

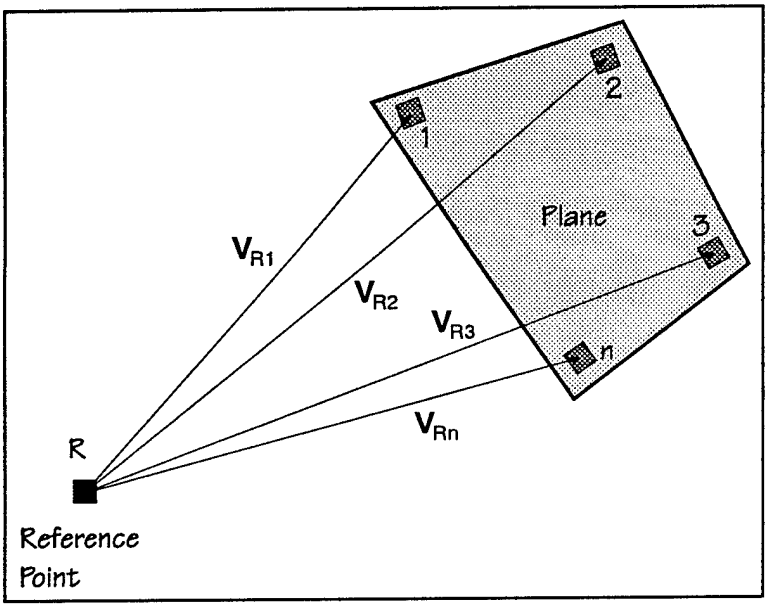

FIGURE 6-1. DIAGRAM OF VECTORS FROM REFERENCE POINT TO EACH POINT ON PLANE

In the figure, the patches on the plane represent either antennas or reflective areas that define the plane. The reference point is used as an absolute WGS 84 reference and also as a reference for the vectors to each patch, such as V_{R1}. If the patches are reflective areas, an auxiliary antenna array (not shown) is needed to select and receive reflections from each area (see Figure 5-2).

The general equation for a plane given in Equation (6-4) is rewritten in Equation (6-5). The coefficients c_x, c_y, c_z are to be estimated from observations of the x_k, y_k, z_k coordinates referred to point R.

$$c_x x_k + c_y y_k + c_z z_k + c_0 = 0 \qquad (6\text{-}5)$$

The least squares formulation proceeds as follows. First, write Equation (6-5) with ϵ_k on the right to acknowledge that each k point will be offset slightly from the true plane. Then square both sides. The result is Equation (6-6).

$$(c'_x x_k + c'_y y_k + c'_z z_k + c'_0)^2 = \epsilon'^2_k \tag{6-6}$$

Notice that both sides of (6-6) can be multiplied by c'^{-2}_0 thereby eliminating that constant. The new coefficients are written without the accent mark in Equation (6-7). In this new form, sum Equation (6-6) over all k and set it equal to E.

$$E = \sum_{k=1}^{n} \epsilon_k^2 = \sum_{k=1}^{n} (c_x x_k + c_y y_k + c_z z_k + 1)^2 \tag{6-7}$$

Then find the partial derivative of E with respect to each of the three coefficients c_x, c_y, c_z. These are listed as Equations (6-8).

$$\begin{aligned}
\frac{\partial E}{\partial c_x} &= 2 \sum_{k=1}^{n} (c_x x_k^2 + c_y y_k x_k + c_z z_k x_k + x_k) \\
\frac{\partial E}{\partial c_y} &= 2 \sum_{k=1}^{n} (c_x x_k y_k + c_y y_k^2 + c_z z_k y_k + y_k) \\
\frac{\partial E}{\partial c_z} &= 2 \sum_{k=1}^{n} (c_x x_k z_k + c_y y_k z_k + c_z z_k^2 + z_k)
\end{aligned} \tag{6-8}$$

In order to find the minimum of E with respect to the coefficients, each of these equations is set equal to zero. Then the right most term is shifted to the right-hand side. The result is shown in Equations (6-9).

$$\begin{aligned}
\sum_{k=1}^{n} (c_x x_k^2 + c_y y_k x_k + c_z z_k x_k) &= - \sum_{k=1}^{n} x_k \\
\sum_{k=1}^{n} (c_x x_k y_k + c_y y_k^2 + c_z z_k y_k) &= - \sum_{k=1}^{n} y_k \\
\sum_{k=1}^{n} (c_x x_k z_k + c_y y_k z_k + c_z z_k^2) &= - \sum_{k=1}^{n} z_k
\end{aligned} \tag{6-9}$$

These are the normal equations that must be solved for the three coefficients. In matrix form, this can

be rewritten as follows: Define an A matrix that contains the coordinates x_k, y_k, z_k for each observation.

$$A = \begin{bmatrix} x_1 & y_1 & z_1 \\ x_2 & y_2 & z_2 \\ x_3 & y_3 & z_3 \\ \vdots & \vdots & \vdots \\ x_n & y_n & z_n \end{bmatrix} \tag{6-10}$$

Define an X vector that will contain the least squares solution for the coefficients.

$$X = \begin{bmatrix} c_x & c_y & c_z \end{bmatrix}^T \tag{6-11}$$

Finally, to form equations like (6-5), the right hand side must be a column vector of -1's. This is written as Equation (6-12).

$$O = [-1 \quad -1 \quad -1 \quad \ldots \quad -1]^T \tag{6-12}$$

Multiplying these together gives Equations (6-13), or in matrix form, Equation (6-14).

$$\begin{aligned} c_x x_1 + c_y y_1 + c_z z_1 &= -1 \\ c_x x_2 + c_y y_2 + c_z z_2 &= -1 \\ c_x x_3 + c_y y_3 + c_z z_3 &= -1 \\ \vdots \qquad\qquad\quad &= \vdots \\ c_x x_n + c_y y_n + c_z z_n &= -1 \end{aligned} \tag{6-13}$$

$$AX = O \tag{6-14}$$

Next, premultiply both sides of (6-14) by A^T and then premultiply both sides of that result by $(A^T A)^{-1}$. This gives the least squares solution for X that is equivalent to solving the system of equations (6-9).

$$X = (A^T A)^{-1} A^T O \tag{6-15}$$

Whether the A matrix is filled with every single relative kinematic solution vector or whether it just consists of the average vectors to each antenna or patch on the plane is a matter for further discussion. If all solutions are placed in the A matrix, it could be a very large matrix having thousands of rows. With just the averages, then the matrix will have as many rows as there are antennas on the plane.

Once the coefficients are found, then the orientation of the plane in WGS 84 space is known. The errors in the determination can be estimated from the covariance and the adjusted residuals. The coefficients are the direction numbers of a line perpendicular to the plane with the origin at the reference point. To fix the plane in absolute space, the coordinates of a point on the plane need to be found. The absolute position of the reference point V_R plus the mean vector from the reference to a particular point on the plane V_{Rk} can be used to establish the absolute geodetic position of the plane. Let the position vector to a particular point k be as in Equation (6-16).

$$V_k = (V_{xRk} + V_{xR})\hat{x} + (V_{yRk} + V_{yR})\hat{y} + (V_{zRk} + V_{zR})\hat{z} \tag{6-16}$$

This point must lie on the plane, so Equation (6-17) must hold. Since c_x, c_y, c_z are known from Equation (6-15), this provides a means to compute c_0, which fixes the plane in space relative to the origin.

$$c_x(V_{xRl} + V_{xR}) + c_y(V_{yRl} + V_{yR}) + c_z(V_{zRl} + V_{zR}) + c_0 = 0 \tag{6-17}$$

The equation for this particular plane is represented by Equation (6-18).

$$c_x x + c_y y + c_z z + c_0 = 0 \tag{6.18}$$

6.3 AN ASTRONOMIC-GEODETIC TRANSFORMATION

The geodetic unit vector normal to the plane represented by Equation (6-18) has components given in Equation (6-19) and the perpendicular distance from the origin to the plane is given in Equation (6-20).

$$\hat{n}_G = \frac{c_x}{\sqrt{c_x^2 + c_y^2 + c_z^2}}\hat{x} + \frac{c_y}{\sqrt{c_x^2 + c_y^2 + c_z^2}}\hat{y} + \frac{c_z}{\sqrt{c_x^2 + c_y^2 + c_z^2}}\hat{z} \tag{6-19}$$

$$d = \frac{c_0}{\sqrt{c_x^2 + c_y^2 + c_z^2}} \tag{6-20}$$

On the plane, the vector joining points 1 and 2 is given by Equation (6-21).

$$V_{G12} = (V_{xR2} - V_{xR1})\hat{x} + (V_{yR2} - V_{yR1})\hat{y} + (V_{zR2} - V_{zR1})\hat{z} \tag{6-21}$$

The corresponding unit vector is given in Equation (6-22).

$$\hat{V}_{G12} = \frac{(V_{xR2} - V_{xR1})\hat{x} + (V_{yR2} - V_{yR1})\hat{y} + (V_{zR2} - V_{zR1})\hat{z}}{\sqrt{(V_{xR2} - V_{xR1})^2 + (V_{yR2} - V_{yR1})^2 + (V_{zR2} - V_{zR1})^2}} \tag{6-22}$$

A second vector in the plane can be obtained by the cross product shown in Equation (6-23).

$$\hat{V}_{G\times} = \hat{V}_{G12} \times \hat{n}_G \tag{6-23}$$

Together, these three unit vectors form a basis for the geodetic coordinate system. A similar basis in the astronomic coordinate system is required to define the transformation matrix T_{AG} between the two systems. When the same three unit vectors are known in both coordinate systems, a general vector V_G defined in the geodetic system is known in the astronomic system as V_A. This is shown in Equation (6-24).

$$V_A = T_{AG} V_G \tag{6-24}$$

In order to compute the required transformation, put the three vectors that sample the space together as columns of a matrix. The same vectors need to be expressed in both coordinate systems. The basic form of the equation is the same as for a vector, as is shown in Equation (6-25). Then postmultiply both sides of Equation (6-25) by M_G^{-1} to solve for the transformation. This is written in detail in Equation (6-26) (Reference 21).

$$M_A = T_{AG} M_G \tag{6-25}$$

$$T_{AG} = M_A M_G^{-1} = \begin{vmatrix} \hat{n}_{Ax} & \hat{V}_{Axl2} & \hat{V}_{Ax\times} \\ \hat{n}_{Ay} & \hat{V}_{Ayl2} & \hat{V}_{Ay\times} \\ \hat{n}_{Az} & \hat{V}_{Azl2} & \hat{V}_{Az\times} \end{vmatrix} \cdot \begin{vmatrix} \hat{n}_{Gx} & \hat{V}_{Gxl2} & \hat{V}_{Gx\times} \\ \hat{n}_{Gy} & \hat{V}_{Gyl2} & \hat{V}_{Gy\times} \\ \hat{n}_{Gz} & \hat{V}_{Gzl2} & \hat{V}_{Gz\times} \end{vmatrix}^{-1} \tag{6-26}$$

7.0 EXAMPLE OF TRANSFORMATION TECHNIQUE

Data obtained during the *Turntable Test* (Reference 22) performed at the Naval Surface Warfare Center, Dahlgren Division (NSWCDD) during February 1994 can be used to demonstrate the determination of a plane using the method outlined in section 6.0. Four receivers collected two-frequency GPS data simultaneously with Trimble 4000 SSE receivers. During the period of time used here, all sites were static. Figure 7-1 illustrates the approximate relative locations of the four sites. Station 6 at Dahlgren, Virginia was selected for the reference site. The other three sites, MBRE, ASTW, and Station P, define a plane whose normal can be found. The ASTW site is about 33 km southwest of the reference site at Corbin, Virginia. The triangle formed by these three points is long and narrow. OTF kinematic positioning can provide vectors between the reference and the other three sites. These three vectors define the plane at each observation time. All the individual solutions can be averaged together or the solutions can be processed in a filter to form one final result. Either way should be equivalent, any differences being dependent upon the weighting given to each time point.

As shown in Figure 7-1, the distances between the reference and Station P is about 1.2 m, between the reference and MBRE, 1.2 km; and between the reference and ASTW, about 33 km. The variation in the components and the length with respect to the mean values are shown for each baseline in Figures 7-2 through 7-4. As expected, the variations are greatest for the longest baseline (Figure 7-4), most likely because of the greater differences in propagation effects between the distant sites. The other two baselines (Figures 7-2 and 7-3) give similar errors, with the variations probably the result of the local multipath effects. The means and the standard deviations about the means as determined from the reference point are listed in Table 7-1. The unit vectors of the means listed in Table 7-1 are shown in Table 7-2. The distance from the reference point along a line perpendicular to the plane is 0.021 m.

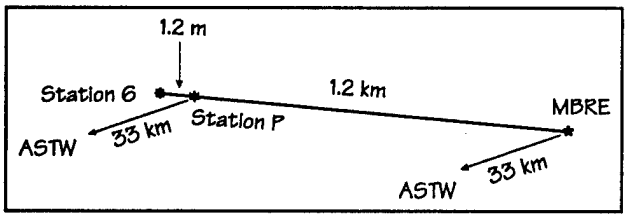

FIGURE 7-1. PLAN DIAGRAM OF FOUR SITES USED FOR TURNTABLE TEST

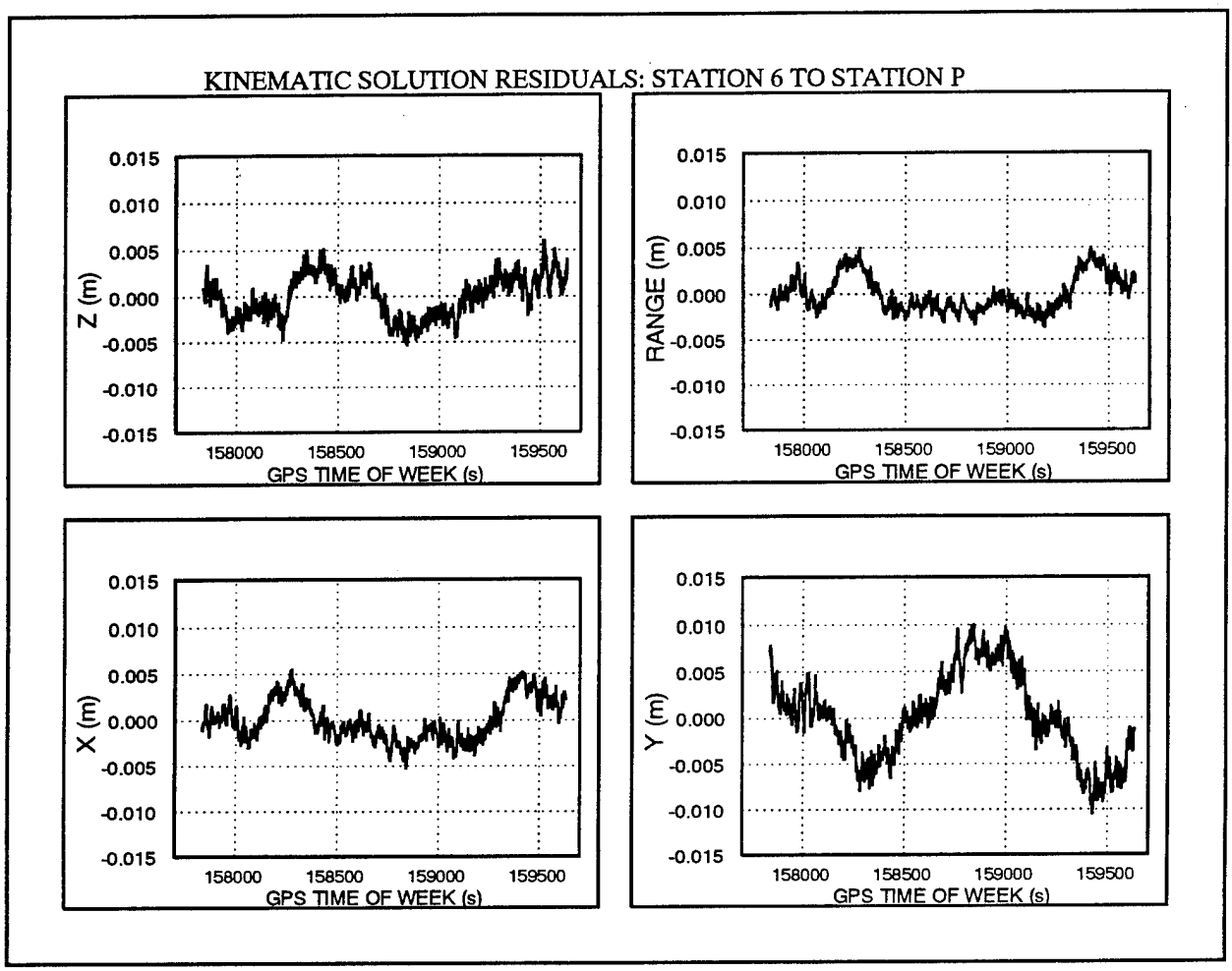

FIGURE 7-2. VARIATIONS IN EACH COMPONENT FROM MEAN SOLUTION FOR REFERENCE SITE TO STATION P

TABLE 7-1. MEAN (η) AND STANDARD DEVIATION (σ) OF SITES WITH RESPECT TO REFERENCE

	X (m)		Y(m)		Z(m)	
	η	σ	η	σ	η	σ
Station 6 to P	1.1814	0.0023	-0.0007	0.0047	-0.3666	0.0023
Station 6 to MBRE	1126.7854	0.0024	-42.8533	0.0040	-369.7550	0.0023
Station 6 to ASTW	-26553.4141	0.0041	-15170.5703	0.0195	-11198.9746	0.0140

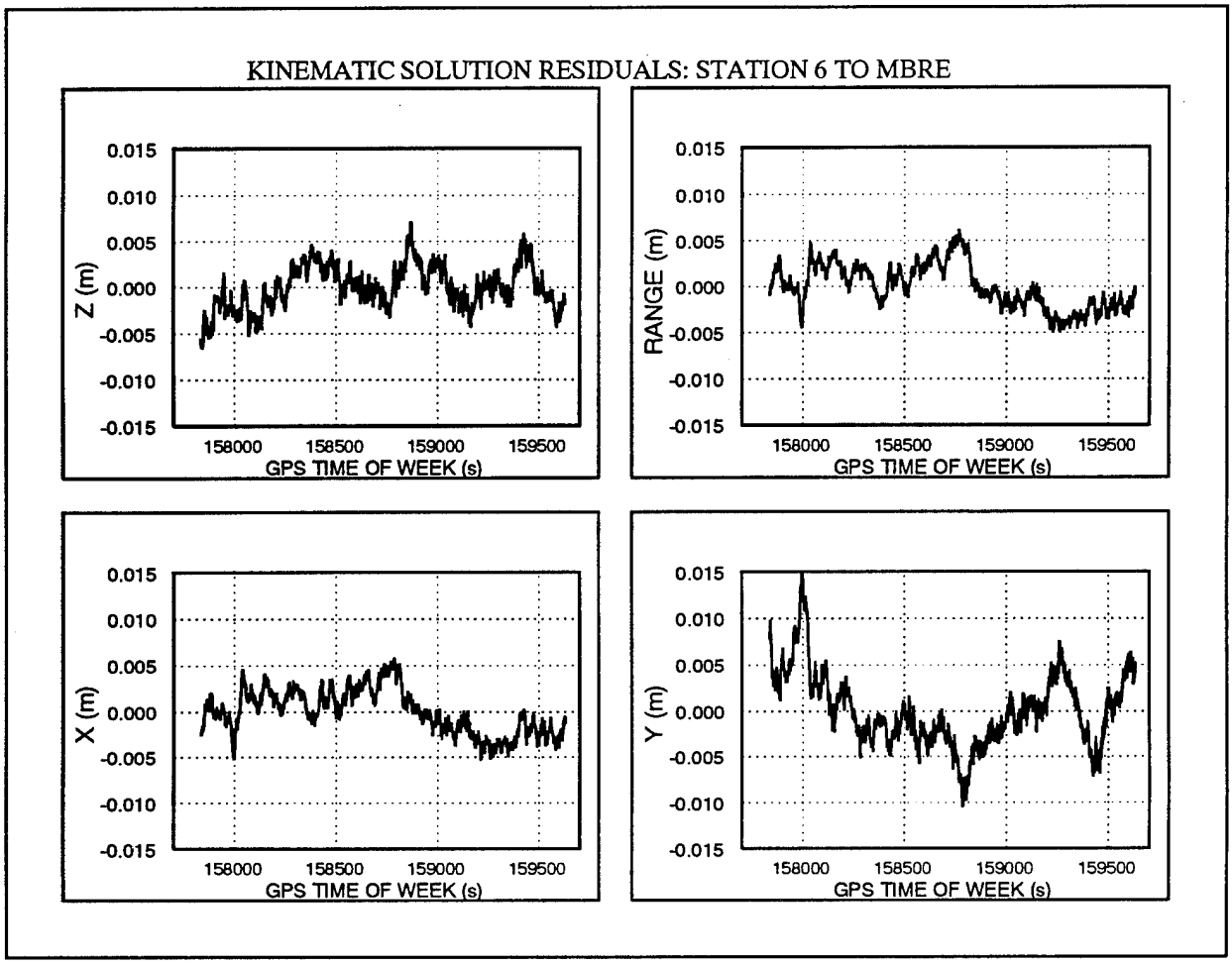

FIGURE 7-3. VARIATIONS OF COMPONENTS FROM MEAN FOR REFERENCE TO MBRE

TABLE 7-2. UNIT VECTORS FOR THREE MEANS LISTED IN TABLE 7-1

Reference to...	X	Y	Z
Station P	0.9551	-0.0006	-0.2963
MBRE	0.9495	-0.0361	-0.3116
ASTW	-0.8153	-0.4658	-0.3439

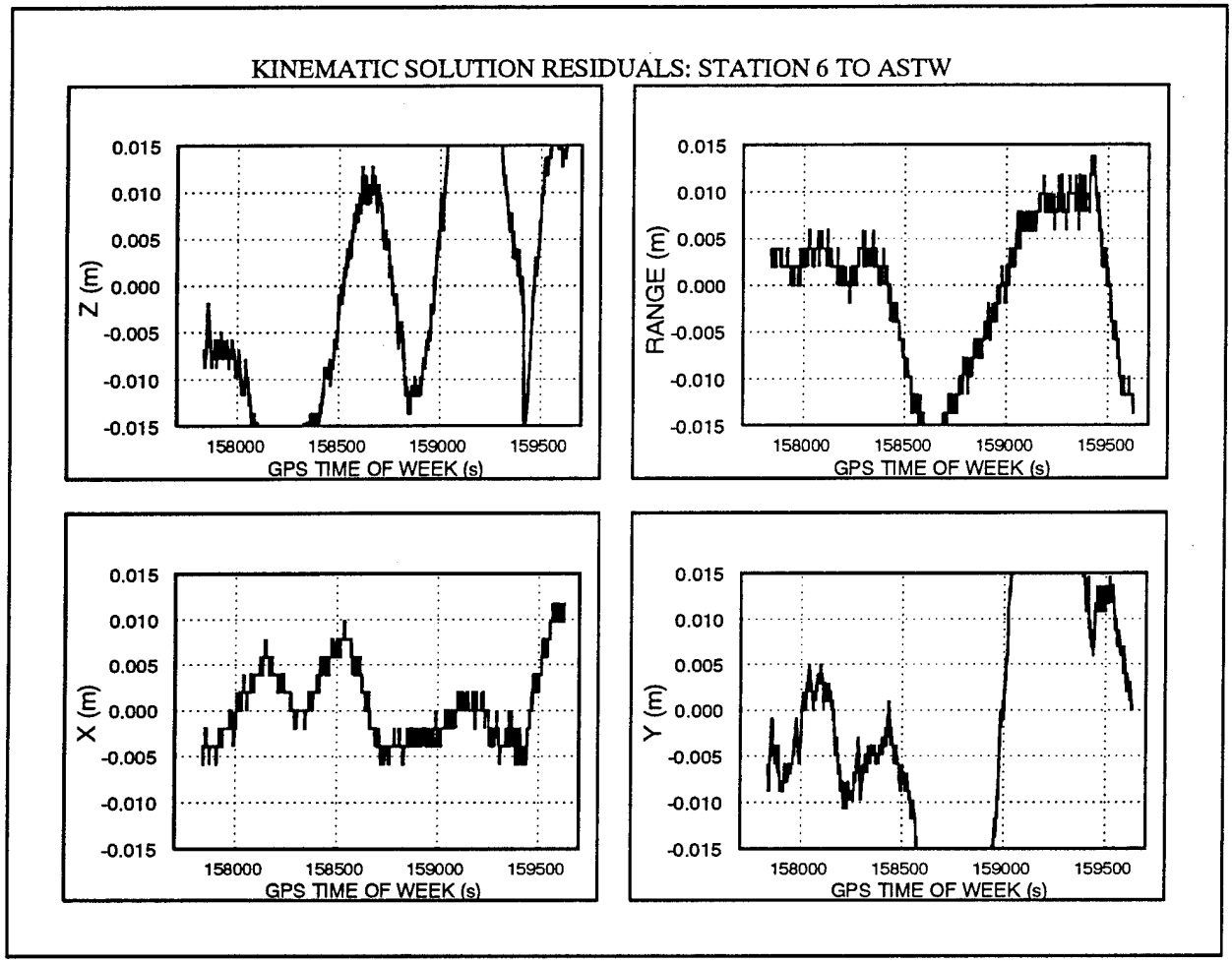

FIGURE 7-4. VARIATIONS OF COMPONENTS FROM MEAN FOR REFERENCE TO ASTW

The mean values define the plane with respect to the reference point. The plane with respect to the WGS 84 origin can be found from Equation (6-16) by adding the absolute position of the reference. The result is listed in Table 7-3. The normal vector to the plane can be computed by Equation (6-19) and the distance from the origin by Equation (6-20). The normal expressed with respect to the reference point and the WGS 84 origin is listed in Table 7-4. The matrices $\boldsymbol{M}_G$ and $\boldsymbol{M}_A$ expressed by Equation (6-25) can be computed as outlined in Equations (6-19), (6-22), and (6-23). The result for $\boldsymbol{M}_G$ is listed in Table 7-5. Then if the same normal vector $\boldsymbol{M}_A$ is known in the astronomic coordinate system, the transformation between them $\boldsymbol{T}_{AG}$ can be found by Equation (6-26).

TABLE 7-3. MEAN VECTORS WITH RESPECT TO WGS 84 ORIGIN

	X (m)	Y (m)	Z (m)
Station P	1123603.9094	-4882075.6937	3934314.9574
MBRE	1124729.5134	-4882118.5463	3933945.5690
ASTW	1097049.3146	-4897246.2667	3923116.3495

TABLE 7-4. UNIT VECTOR NORMAL TO PLANE DEFINED BY STATION 6, MBRE, AND ASTW

Unit Vector			Perpendicular Distance (m)	
X	Y	Z	Reference	Origin
0.174685	-0.764139	0.620948	0.021	6369867.214

TABLE 7-5. MATRIX M_G DEFINING GEODETIC SPACE

X	Y	Z
0.174685	0.949524	0.260556
-0.764139	-0.036149	0.644038
0.620948	-0.311604	-0.719254

The variation of the baseline components in time, shown in Figures 7-2 through 7-4, results in a variation in the definition of the plane and its normal about the mean value. This can be expressed as an angular movement of the normal vector in each of the three components. The standard deviation of the normal is listed in Table 7-6 for the components and the root-sum-of-squares (RSS). The time variation is plotted in Figure 7-5. It is immediately clear that the variation is not entirely noise, but contains a slowly varying time-dependent offset. This residual is probably due to propagation effects including multipath as mentioned previously. It would be desirable to test this hypothesis by checking the repeatability of the vector motion from day to day. If repeatability can be demonstrated, then averaging across days at specific times having the same satellite geometry may offer a more precise way to establish the normal vector than averaging within a day.

TABLE 7-6. MEAN (η) AND STANDARD DEVIATIONS (σ) OF EACH COMPONENT OF NORMAL VECTOR

Units = arcsec	X	Y	Z	RSS
η	0	0	0	1.190
σ	0.845	0.650	1.034	0.888

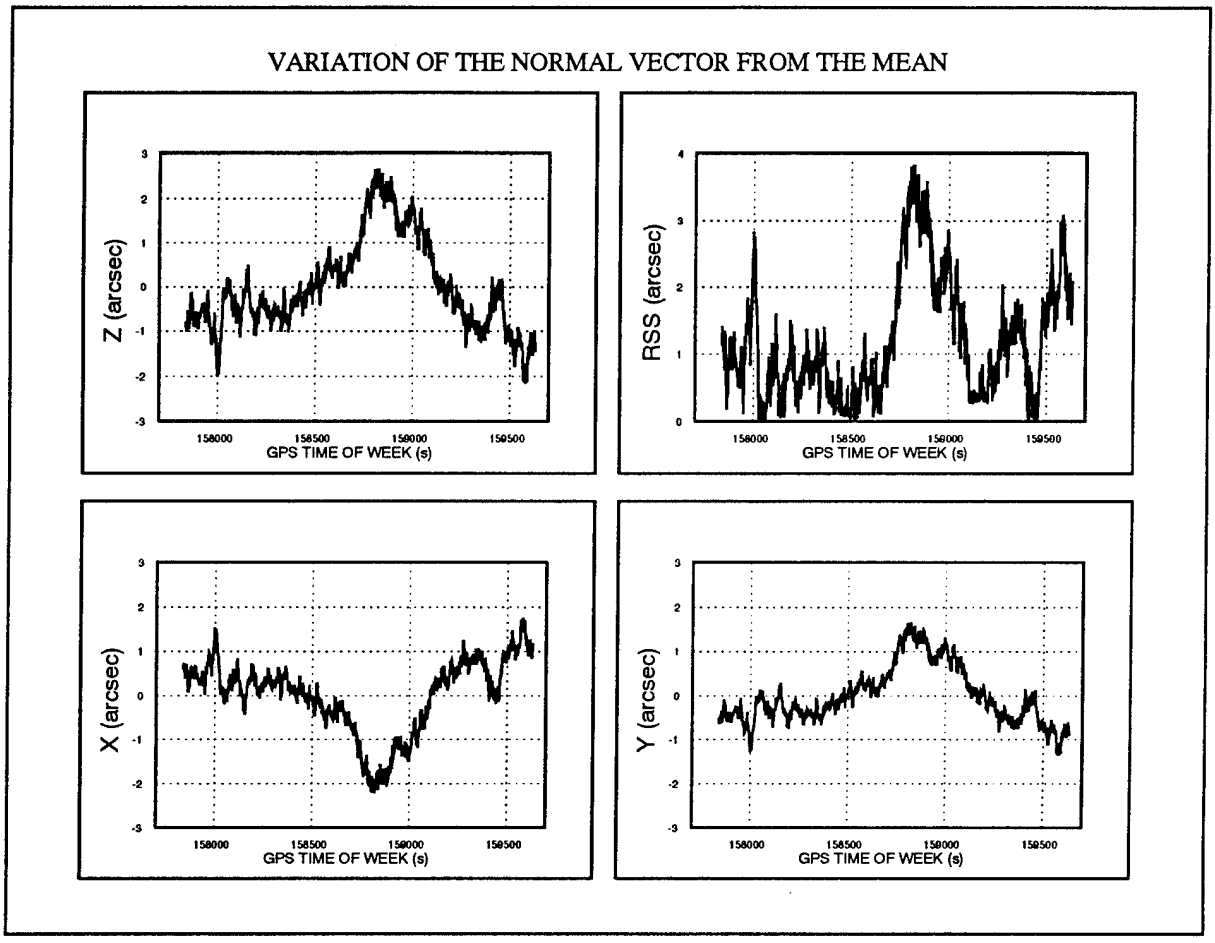

FIGURE 7-5. VARIATION OF COMPONENTS OF NORMAL VECTOR

8.0 POSSIBLE PAR IMPLEMENTATION

The determination of a plane in space assumes that the plane is directly defined at three or more points by GPS antennas or indirectly defined by reflections off the plane at three or more points that are received at an auxiliary antenna array. The observation equations were described in section 5.0. Successful reception of indirect signals is dependent upon several factors, including the effective target cross-section, the distance from the target to the receiving antenna, the gain of the receiving antenna, and the ratio of the strength of the direct signal to the indirect signal at the receiver.

Once signals are received, the PAR application requires that repeatability and accuracy be maintained at an extremely high level. Small uncorrected biases will invalidate the results. In order to achieve the required performance, there are two requirements that must be met simultaneously. The indirect signals must be detectable and usable at the sensor, and the sensor biases must be predictable and correctable.

8.1 RADAR RANGE EQUATION

The effective GPS C/A signal power at the surface of the earth is P_{GPS}= −163 dBw (Reference 23). After reflection from a surface and propagation to a receiving antenna, the power available would likely be smaller unless the reflecting surface has strong focusing properties. The effect of reflection can be modeled by the radar range equation. The form of this equation will be developed and discussed with respect to the PAR application.

Two important relationships between wavelength λ, antenna physical area A, antenna gain G_A, and beam solid angle Ω_A need to be introduced first. The first relationship relates wavelength to area and solid angle, and the second relationship defines gain as inversely proportional to solid angle. These are shown in Equations (8-1) and (8-2).

$$\lambda^2 = A\,\Omega_A \tag{8-1}$$

$$G = \frac{4\pi}{\Omega_A} \tag{8-2}$$

As shown in Equation (8-2), since the solid angle Ω_A cannot exceed 4π, the gain cannot be less than unity. If the two equations are merged by elimination of the solid angle, the result is Equation (8-3).

$$A = \lambda^2 \frac{G}{4\pi} \tag{8-3}$$

The first step toward the radar equation is the Friis transmission formula (Reference 24). At a distance r_1 from the transmitter, the power received is equal to the product of the power density $\tilde{P}_R$ and the area of the receiving antenna, as expressed in Equation (8-4).

$$P_R = \tilde{P}_R A \tag{8-4}$$

The power density is defined by the power per unit area impinging on the inside surface of a sphere of radius r_1. If the transmitting antenna gain, G_T, is unity, then the power density is the same everywhere on the surface of the sphere. If G_T is a function of direction, then the maximum power density is where G_T is maximum. The power density is given by Equation (8-5).

$$\tilde{P}_R = \frac{G_T P_T}{4\pi r_1^2} \tag{8-5}$$

Since it is better to write the radar equation in terms of wavelength rather than area, the A in (8-4) can be removed by substituting Equation (8-3). The result is Equation (8-6).

$$P_R = \tilde{P}_R \frac{\lambda^2 G_R}{4\pi} \tag{8-6}$$

If Equation (8-5) is substituted into Equation (8-6) the result is the Friis transmission formula, Equation (8-7). In the general case where the gains are functions of direction, the power received is also a function of direction.

$$P_R = \left[\frac{\lambda}{4\pi r_1}\right]^2 G_R G_T P_T \tag{8-7}$$

This equation states that the power received at a receiver is proportional to the power transmitted times the transmitter antenna gain times the receiver antenna gain and is inversely proportional to the square of the separation distance. This equation assumes free space propagation and that the antenna gains are maximum; that is, they both favor the direction along the line joining the transmitter to the receiver. Written in logarithmic form as decibels, where $dB = 10 \log_{10} \frac{P_2}{P_1}$, the formula in Equation (8-7) becomes a sum in Equation (8-8).

$$P_R = 20\,[\log \lambda - \log (4\pi) - \log r_1] + 10\,[\log G_T + \log G_R + \log P_T] \quad \text{dBw} \qquad (8\text{-}8)$$

In the case of GPS, the part pertaining to the transmitter can be lumped together into the P_{GPS} referenced above. That is, the first three terms on the right and the terms involving G_T and P_T can be combined. The simplified equation is shown as Equation (8-9). This confirms what is already well known, that the only way for a user to increase the signal at the receiver is to add gain at the receiving antenna.

$$P_R \approx P_{GPS} + 10 \log G_R \quad \text{dBw} \qquad (8\text{-}9)$$

To continue development of the radar range equation, Equation (8-5) is rewritten to represent the power density incident on a reflecting surface at a distance r_1 from the transmitter. This is shown in Equation (8-10).

$$\tilde{P}_{R1} = \frac{G_T P_T}{4\pi r_1^2} \qquad (8\text{-}10)$$

At the reflecting surface, some of this incident energy, $\sigma \tilde{P}_{R1}$, is reradiated in a direction toward a receiving antenna at a distance r_2. The symbol σ represents the radar cross section of the reflecting surface and has units of m^2. Therefore the power density received at the antenna a distance r_2 from the reflector is represented by Equation (8-11).

$$\tilde{P}_{R2} = \frac{\sigma \tilde{P}_{R1}}{4\pi r_2^2} \qquad (8\text{-}11)$$

Finally, (8-10) can be substituted into (8-11) and the result multiplied by the receiver antenna area A_{R2}, as expressed by Equation (8-3), to change from power density to power. The result of these substitutions is a form of the radar range equation (Reference 25) shown as Equation (8-12).

$$P_{R2} = \frac{\sigma \lambda^2 G_T G_{R2}}{(4\pi)^3 r_1^2 r_2^2} P_T \qquad (8\text{-}12)$$

The reflected power received at point *2* is directly proportional to the power transmitted, the radar cross section, the wavelength squared, and the product of the antenna gains at the transmitter and receiver. The received power is inversely proportional to the product of the squares of the distances from transmitter to reflector and from reflector to the receiving antenna. This equation can also be written in decibels in the same manner as Equation (8-8), as shown in Equation (8-13).

$$P_{R2} = 20\,(\log \lambda - \log(4\pi) - \log r_1 - \log r_2) + 10\,(\log \sigma - \log(4\pi) + \log G_{R2} + \log G_T + \log P_T) \quad \text{dBw} \tag{8-13}$$

As before, the terms dealing with the transmitter can be lumped together and replaced by P_{GPS}. The resulting simplified form is displayed as Equation (8-14).

$$P_{R2} \approx P_{GPS} - 20 \log r_2 + 10[\log G_{R2} + \log \sigma - \log(4\pi)] \quad \text{dBw} \tag{8-14}$$

The parameters remaining that can be adjusted include the distance between the reflector and the receiving antenna, the receiving antenna gain, and the radar cross section of the reflector. In order to use kinematic relative positioning to determine the orientation of the target plane, the receiver must be able to track the satellites with the indirect signals in much the same manner as it does with direct signals. This requires that the losses in Equation (8-14) due to reflection, reradiation, and reception at a point r_2 meters distant be made up by the antenna gain and the radar cross section. The constant 4π contributes -11 dB, while the other parameters can be chosen as part of the design.

As an example, suppose that the range r_2 is 10 m (-20 dB), the antenna gain is 20 dB, and the radar cross section is selected as 10 m^2 (10 dB). Figure 8-1 shows that the power received indirectly amounts to only a 1-dB reduction in signal strength compared to the direct signals. It is clear from this choice of parameters, however, that the radar cross section cannot equal the physical cross section. The physical cross section of the entire window will be smaller than 1 m^2, and the points used to determine the plane may be on the order of 1 cm^2. In order to achieve the large radar cross section, it will be necessary to enhance the reflective areas by some method in order to increase its apparent size. This may require a physical modification or addition to the window's surface. To achieve the high antenna gain, an elaborate receiving antenna array is required. The combination of the 20-dB gain antenna and the enhanced radar cross section will likely increase the system sensitivity to antenna phase center errors (Reference 26). A phase center correction table could be developed and used to correct the observed ranges for phase center variations as a function of satellite direction. Empirical verification of this technique will be needed to establish that the required millimeter accuracy can be achieved. Development of the antenna and the cross section enhancement will be easier to accomplish at a single frequency. Therefore only L_1 operation is recommended.

8.2 ADAPTIVE PHASED ARRAY ANTENNA

For signal strength purposes, it is important to have a high gain antenna. High gain implies directionality, which would be necessary in any event to help reduce the direct signal strength. A fixed array would not be suitable for the PAR application because the direction to the satellites constantly changes. A phased array (Reference 27) would be better suited because the direction of the nulls could be managed to follow the satellites across the sky, thus reducing the direct signals by an amount equal to the null depth. An array of *n* antennas can produce *n-1* nulls.

If the best four satellites were constantly tracked, an array with a minimum of five antenna elements is required for PAR. Since the pseudorange code provides discrimination between satellites, the direct signals from the satellites not being tracked will not interfere and do not have to be nulled. Simultaneous reception from the several enhanced areas on the target plane would require multiple phased arrays. Otherwise, with only one phased array antenna, the enhanced areas could be targeted in a predetermined sequence over a period of time.

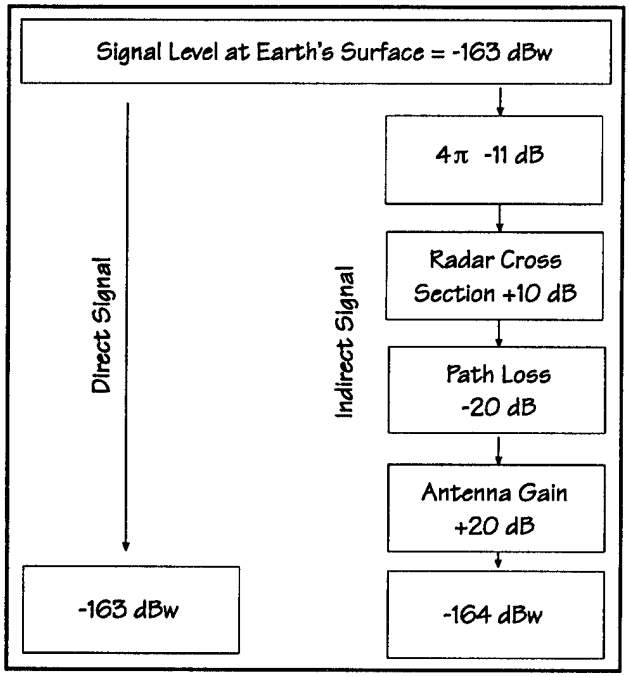

FIGURE 8-1. SIGNAL GAINS AND LOSSES BY INDIRECT PATH COMPARED TO DIRECT PATH

A computerized controller for the phased array would need to be developed. It would select the satellites to be observed, or alternately poll the receiver for satellites to be nulled. A single frequency geodetic quality receiver could be used without modification if it supported the relevant input and output data. The controller allows flexibility since it would be directed by software. It could also be used to receive data from the direct signal reference antenna and could do the kinematic relative position solutions in near real time.

8.3 MULTISTATIC RADAR

A receiver could be specifically designed to detect the indirect signal by taking advantage of the fact that it always arrives later than the direct signal. If the GPS satellites are considered as wideband noise sources, then the application becomes very much like a multistatic radar system, but one where the transmitter is not under direct control of the user. With a receiver capable of cross correlating the

direct and indirect signals, an observation of the relative time delay is obtained. Since the motion of the satellites is well known, and with the target and the receiving antenna stationary, the satellite motion can be computed and compensated. Then long integration times over several seconds become possible, and the requirements for a high gain receiving antenna and the enhanced radar cross section at the target are lessened. However, a phased array capable of deep nulls will likely be required to help keep the direct signal out of the indirect signal channel in any case.

A multistatic radar system can collect three classes of observations: time delay, Doppler frequency, and angular space coordinates. The time delay is due to the different path lengths taken by the direct and indirect signals. The Doppler frequency is proportional to the velocity of the satellite, the target, or the receiver projected on the line of sight joining them. The angular space coordinates depends upon the directional characteristics of the antenna array. The time delay would be the primary observation of interest in this case since the target and receiver are stationary and the motion of the satellite is already known, as noted above. There is an interesting possibility that the Doppler could be used as a means of identifying the target signal.

If a small facetted rotating cylinder were constructed that could be attached to the target, its rotation would impress itself as a periodic Doppler shift onto the indirect signal. Since the period of rotation would be known, the corresponding Doppler frequency could be searched for that signal. The frequency offset would be nonzero, and therefore most of the zero Doppler clutter reflections would be removed by Doppler frequency filtering. Multiple targets could be simultaneously accommodated if the frequencies were different. This could provide a significant increase in signal-to-noise and make the individual target signals unambiguous.

9.0 CONCLUSIONS

A technique to generate a transformation between the astronomic and geodetic reference frames has been described. The technique is based on knowing the orientation of a plane in both frames. There are advantages to this technique over the conventional method, which requires measurements of the deflection of the vertical. Employing an astrolabe to measure the deflection of the vertical insures high accuracy transformations, but obtaining precise measurements is time-consuming. Additionally, the measurements must be made *in situ*, which may be impractical. The proposed technique may potentially overcome both of these difficulties. Defining an astronomic-geodetic transformation for a laboratory window at Holloman Air Force Base was the specific problem addressed in this report. The astronomic orientation of the window was assumed known. The window's geodetic orientation may be determined using GPS kinematic relative positioning.

GPS kinematic relative positioning using phase observations offers millimeter accuracy. Over short baselines, ionospheric effects are mostly removed by differencing. Double differencing between the receivers and the satellites removes the clock effects of both, and is considered the best mode of processing. Single frequency solutions are most desirable because of the their low-noise characteristics. The proposed method for positioning the window at Holloman AFB employs GPS multipath signals. Using the indirect signal introduces an effect similar to a local clock offset and so does not complicate the data analysis procedure.

Using data from a static relative positioning test, the level of uncertainty with which a plane's orientation can be determined using GPS data was estimated. The estimated uncertainty realized using direct signals, about 1.0 arcsec, is too large for generating useful transformations for the PAR. Systematic noise effects present in results may be diminished or removed by repeated observation or other noise reducing methods thereby improving the plane's orientation uncertainty. It is anticipated that results generated using indirect signals will contain more noise.

The power of the indirect signal from the window will be less than that of a direct signal. To compensate, either physical modifications, or additions to the window, or high-gain antenna arrays are required. In this case, high-gain receiving antennas are needed to reject the unwanted direct signal and to make up some of the loss due to the indirect path. Additional augmentation of the radar cross section at the reflecting surface is also required. With suitable attention to the gains and losses along the indirect path, an unmodified geodetic-quality receiver could be used to collect the pseudorange and phase observations in the same manner as for the direct signals. The antenna design is critical for this option, and a phased array would be required to form nulls in the direction of the direct signals from the constantly moving satellites. Simultaneous observations from several reflecting points could be accomplished if several phased array antennas and receiver combinations were used. It would be possible to direct the phased array at the several reflective points in sequence, but it is unlikely that the main beam of the array would be narrow enough to effectively discriminate between them. Therefore only one reflective surface can be made visible at a time.

Instead of employing a geodetic GPS receiver, a wideband correlating receiver could be designed and used with the phased array. In this case, the system becomes a multistatic radar using the GPS satellites as sources of illumination. Since the satellite motion can be compensated, long integration times are possible, and the antenna forward gain and target cross section requirements may be relaxed. However, the direct signals still need to be nulled by the phased array to prevent them from interfering with the desired indirect signals.

Physically mounting GPS antennas on the target is the cheapest option, but sub-arcsec absolute accuracy will need to be demonstrated. The antenna phase centers need to be calibrated. The indirect option using a geodetic GPS receiver requires the development of a phased array antenna and target cross section enhancers. The multistatic radar option requires the phased array antenna, the target cross section enhancers, plus the development of a wideband correlating receiver and the necessary software for data analysis. The accuracy of this last option will probably not be as good as the first two options because the phase observations may not be recovered. All options will require that prototype equipment be developed and extensively tested in a controlled environment.

10.0 RECOMMENDATIONS

Single frequency operation is recommended both for lower noise observations and for easier antenna design. Since direct mounting of antennas on the target is not allowed, using indirect signals and a GPS geodetic receiver is recommended. Considerable antenna development will be required. The antenna phase center stability will be a requirement for all options. The phase centers of existing antennas for the direct signal option and for use as elements of the phased array can be tested in anechoic chambers and/or with real signals in an out-of-doors environment. Both types of testing may be required to establish and understand the relevant properties.

For the recommended indirect options, a phased array design proposal can be developed with array analysis software to determine the number of antenna elements needed and their geometrical arrangement. The null performance and precision with which each element's phase shifter has to be controlled are also important. The motion of the effective array phase center will need to be established as a function of the number of nulls and their directed positions.

The development of high cross section targets that can be attached to selected points of the target plane need development. These may consist of foil dipole strips terminated so that most incident energy is returned to the phased array, giving them a cross section larger than their physical dimension. The rotating cylinder suggested for the multistatic radar option will probably not be useful with the geodetic receiver since it will just add a constant Doppler frequency offset that will be removed in the doubly differenced observations.

Experiments with the direct signal method with multiple receivers and antennas should be pursued to establish the best orientation accuracy that can be expected from GPS observations. Various averaging schemes could be tested to remove noise and compensations or special bias parameters inserted in the analysis software in an effort to solve for and remove the system biases.

11.0 REFERENCES

1. Roth, B., Subj: GPS Radar, DMA Memorandum, Defense Mapping Agency Systems Center, Washington, DC, 1 Mar 1994.

2. Hoffmann-Wellenhof, B.; Lichtenegger, H.; and Collins, J., *GPS Theory and Practice*, Springer-Verlag Wien, New York, 1994.

3. Ware, R., "Global Positioning Finds Applications in Geosciences Research," *EOS, Transactions, American Geophysical Union*, Vol. 76, No. 18, 2 May 1995, p. 187.

4. Genrich, J. F. and Bock, Y., "Rapid Resolution of Crustal Motion with Short-Range GPS," Journal of Geophysical Research, Vol. 97, No. B3, 1992, pp. 3261-3269.

5. Hermann, B., "Locating Passive Targets Using Scattered Energy Originating from the Global Positioning System," NSWCDD, Dahlgren, VA, 2 Feb 1994.

6. Heiskanen, W. A. and Moritz, H., *Physical Geodesy*, W.H. Freeman and Company, San Francisco, 1967.

7. Kumar, M., "World Geodetic System 1984: A Modern and Accurate Global Reference Frame, "Marine Geodesy, Vol. 12, 1988, pp. 117-126.

8. *Department of Defense World Geodetic System 1984, Its Definition and Relationships with Local Geodetic Systems*, DMA TR 8350.2, 30 Sep 1987, Washington, DC .

9. Decker, B. L., "World Geodetic System 1984," *Proceedings of the Fourth International Geodetic Symposium on Satellite Positioning*, Austin, TX, Apr 1986, Vol. 1, pp. 69-92.

10. Malys, S. and Slater, J. A., "Maintenance and Enhancement of the World Geodetic System 1984," *Proceedings of ION GPS-94, 7th International Technical Meeting of the Satellite Division of the Institute of Navigation*, Salt Lake City, UT, Sep 1994, pp. 17-24.

11. Swift, E. R., et al., *GPS Orbit Estimation and Station Coordinate Improvement Using 1992 IGS Campaign Data Set*, NSWCDD/TR-94/267, Oct 1994, Dahlgren, VA.

12. Braasch, M. S., "A Signal Model for GPS," *NAVIGATION*, Vol. 37, No. 4, Winter 1990-1991, pp. 363-377.

13. Melbourne, W. G., "The Case For Ranging In GPS-Based Geodetic Systems, " *Proceedings of the First International Symposium on Precise Positioning with the Global Positioning System*, Rockville, MD, Apr 1985, pp. 373-386.

14. Hatch, R., "The Synergism of GPS Code and Carrier Measurements, " *Proceedings of the Third International Geodetic Symposium on Satellite Doppler Positioning*, New Mexico States University, Feb 1982, Vol. 2, pp.1213-1231.

15. Abidin, H., "Extrawidelaning For 'On-The-Fly' Ambiguity Resolution: Simulation of Multipath Effects," *Proceedings of ION GPS-90*, Colorado Springs, CO, Sep 1990, pp. 525-533.

16. Evans, A. G., "Comparison of GPS Pseudorange and Biased Doppler Range Measurements to Demonstrate Signal Multipath Effects," *Proceedings of the Fourth International Geodetic Symposium on Satellite Positioning*, Austin, TX, Apr 1986, Vol.1, pp. 573-587.

17. Remondi, B. W., *Using the Global Positioning System (GPS) Phase Observable for Relative Geodesy: Modeling, Processing, and Results*, Ph.D. Dissertation, The University of Texas at Austin, May 1984, Chapter 3.

18. Clynch, J. R. and Coco, D. S., "Error Characteristics of High Quality Geodetic GPS Measurements: Clocks, Orbits, and Propagation Effects," *Proceedings of the Fourth International Geodetic Symposium on Satellite Positioning*, Austin, TX, Apr 1986, Vol. 1, pp. 539-556.

19. Gourevitch, S., "Implications of 'Z' Technology for Civilian Positioning," *Proceedings of ION GPS-94, The 7th International Technical Meeting of The Satellite Division of The Institute of Navigation*, Salt Lake City, UT, Sep 1994, pp. 149-155.

20. Remondi, B. W., Subj: Kinematic GPS Results Without Static Initialization, NOAA Technical Memorandum NOS NGS-55, Rockville, MD, May 1991.

21. Kleusberg, A., "Mathematics of Attitude Determination with GPS," *GPS WORLD*, Vol. 6, No. 5, Sep 1995, pp.72-78.

22. Hermann, B. R., et al., "Kinematic On-The-Fly GPS Positioning Relative to a Moving Reference," *Proceedings of ION GPS-94, 7th International Technical Meeting of the Satellite Division of the Institute of Navigation*, Salt Lake City, UT, Sep 1994, pp. 1499-1507.

23. Spilker, J. J., Jr., "GPS Signal Structure and Performance Characteristics," *Global Positioning System*, The Institute of Navigation, Washington, DC, Vol. 1, 1980, pp. 29-54.

24. Johnson, Richard C., *Antenna Engineering Handbook*, 2nd Edition, McGraw-Hill, New York, 1984, Chapter 1.

25. Stimson, George W., *Introduction to Airborne Radar,* Hughes Aircraft Company, El Segundo, CA, 1983.

26. Tranquilla, J. M., "Multipath and Imaging Problems in GPS Receiver Antennas," *Proceedings of the Fourth International Geodetic Symposium on Satellite Positioning*, Austin, TX, Apr 1986, Vol. 1, pp. 557-571.

27. Hudson, J. E., *Adaptive Array Principles*, Institution of Electrical Engineers, Peter Peregrinus Ltd., London, U.K., 1989.

APPENDIX A

IMPROVING THE PRECISE AZIMUTH REFERENCE (PAR)

A requirement has been established to improve the accuracy of the PAR. Currently maintained by DMA at an accuracy approaching 0.1 arcsec, the improved accuracy will approach 0.01 arcsec. Improving the accuracy of the PAR is a difficult task. In the main body of this report, a multipath tracking technique is proposed to determine the orientation of a plane. Using a similar technique to accurately determine a position on a plane may be a method to improve the PAR's accuracy. A simplified analysis of the magnitude of the errors associated with using the indirect signal tracking technique for PAR improvement is presented below. Further, two other ideas are presented that may hold promise of achieving the order-of-magnitude improvement sought.

To estimate the errors associated with positioning a target using indirect signal tracking, a sensitivity analysis was performed. The range from the antenna (B) (see Figure 5-2) to the target (T) is given in Equation (A-1). The first term on the right-hand side approximates the indirect range from the satellite to the antenna at B via the reflecting target. For this analysis, the range to the satellite from the antenna at B is assumed equal to the range to the satellite from the reflecting surface. The second term of the right-hand side represents the range derived from the direct signal received at antenna B.

$$\rho_{BT.i} = (r^{j}_{B.i} + r_{BT.i}) - r^{j}_{B.i} \qquad \text{(A-1)}$$

The uncertainty in positioning the target is approximated by Equation (A-2). The first term represents the contribution of the absolute uncertainty of satellite position, and the second term is that of the antenna's position. The uncertainties contributed by the satellite and station clocks are assumed negligible over the small distances that multipath tracking is possible. The contribution of the antenna phase center bias is ignored in this equation.

$$\sigma_{BT} = \frac{d(\rho_{BT..})}{dr^{j}_{...}} \sigma^{j} + \frac{d(\rho_{BT..})}{dr_{B..}} \sigma_{B} \qquad \text{(A-2)}$$

Equation (A-2) assumes the target's position uncertainty is a function only of the uncertainty in the satellite and antenna positions and the uncertainty in the antenna-target baseline. The uncertainty in the antenna-target baseline is implicit in the second term of Equation (A-2). A small change in the antenna-target baseline corresponds to a small change in the antenna's position. Equation (A-3) shows the full expression for the partial derivative of the second term of Equation (A-2).

$$\frac{d(\rho_{BT..})}{dr_{B..}} = \frac{d(\rho_{BT..})'}{dr_{B..}} + \frac{d(\rho_{BT..})}{dr_{BT..}} \frac{d(r_{BT..})}{dr_{B..}} \qquad \text{(A-3)}$$

Presented in Table A-1 are three cases representing varying uncertainties for satellite and receiver antenna positions and the resulting uncertainties in the target position. The target's position uncertainties are converted from cm to arcsec by assuming all the resulting uncertainty is perpendicular to the direction of the baseline. The results of the first case show that under the

system's current accuracy, the uncertainty in positioning the reflecting surface over a 25-m baseline is about 74 arcsec. The results of the second case show the small effect the satellite position errors have on the target's position uncertainty. When the satellite position errors decrease from 2 m to 10 cm, no significant improvement occurs in the target baseline uncertainty. The third case represents the projected system accuracy of the near future. In the third case the uncertainty in the station antenna's position decreases from 10 cm to 1 cm and the resulting target position uncertainty improves by an order of magnitude. Because these estimates are for a single measurement, some improvement can be expected with more measurements. However, increasing the number of measurements alone will not satisfy the 0.01 arcsec PAR requirement.

TABLE A-1. POSITIONING A REFLECTING SURFACE OVER A 25 M BASELINE

Assumed			Resulting
Sigmas	Satellite Position (σ_j)	Antenna Position (σ_B)	Target Position (σ_{BT})
Case 1	2 m	10 cm	0.9 cm (74 arcsec)
Case 2	10 cm	10 cm	0.9 cm (74 arcsec)
Case 3	10 cm	1 cm	0.09 cm (7 arcsec)

The receiver's antenna phase center bias was omitted from the above analysis. The physical center of a GPS antenna does not coincide with the point at which the signal is received. The reference point for the signal measurements is the apparent electrical center of the antenna, namely the phase center. The phase center location depends on the signal frequency, the antenna design, and the elevation and azimuth of the satellite. This small bias cannot be ignored when sub-millimeter accuracy is required. The antenna phase center bias contributes at least 1 mm and possible more (5 mm) (Reference A-1) to the position uncertainty of the reflecting surface. It may be possible to eliminate the antenna bias using a technique described by Hermann (Reference A-2).

STAR CATALOGS

The current technique of determining the PAR uses astronomic measurements of the star Polaris. The most accurate star catalog presently available is the Fifth Fundamental Catalog (FK5 Part I). The errors quoted in the catalog indicate the average errors should be about 0.03 arcsec. However, the errors could be as large as 0.1 arcsec especially in the Southern Hemisphere. The U. S. Naval Observatory (USNO) is currently compiling the Washington Fundamental Catalog (WFC), a replacement for the FK5. Unlike FK5, which was a refinement of its predecessor FK4, the WFC will be a new reference frame definition. The WFC will incorporate the best of modern observational catalogs and is expected to contain about 40,000 stars. The WFC will maintain an accuracy of 0.05 arcsec for 10 or more years. It should be available in 1997 (Reference A-3). Employing the WFC in PAR determination should improve its accuracy.

OPTICAL OBSERVATION OF GPS

It may be possible to use optical measurements of the GPS satellites to improve the PAR. The position of the optical center of a GPS satellite can be determined to about 1.25 m, which corresponds to a 0.01-arcsec line of sight accuracy (Reference A-4). This assumes the accuracy of the GPS precise ephemeris to be around 25 cm (Reference A-5), errors in the observer's position to be centimeter level, and errors in calculating the displacement from the satellite center of mass to center of light to be about 1 m (Reference A-4). Improvements in the modeling of reflectance may significantly lower the optical positioning error. To employ this technique, the GPS satellites must be observable through the limited field of view of the laboratory window at Holloman AFB. The altitude* of Polaris at Holloman AFB is about 32.5 deg while that of the GPS satellites is about 60 deg. GPS satellites are approximately magnitude 9 brightness and are observed optically by employing a charge-couple device (CCD). Figure A-1 shows an example of a CCD image of PRN 27. The 5-sec exposure taken with a 0.5-m telescope on 16 August 1993 at the Zimmerwalÿd Observatory of the University of Bern, Switzerland (Reference A-6). Installing the necessary equipment to obtain optical images may not be feasible in the laboratory at Holloman AFB.

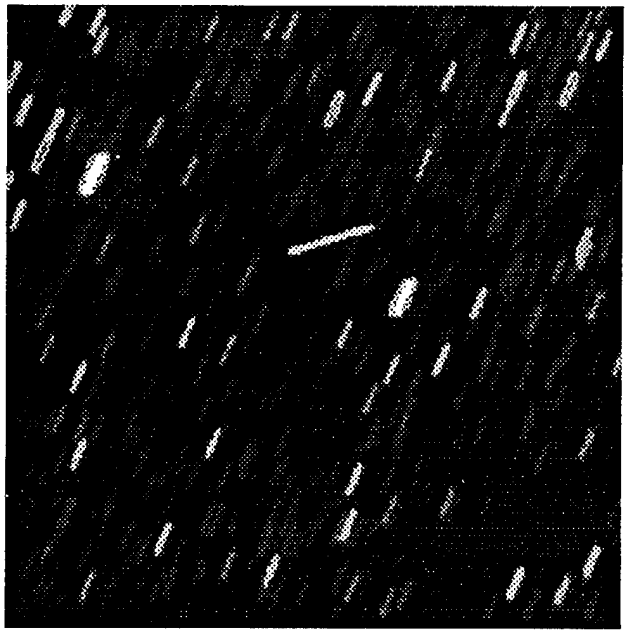

FIGURE A-1. A 5-SEC CCD IMAGE OF PRN 27 TRAVERSING THE CONSTELLATION CYGNUS ON 16 AUGUST 1993 TAKEN AT THE ZIMMERWALŸD OBSERVATORY. FIELD OF VIEW IS 17' BY 17'

* Altitude is the angular distance above the horizon measured on the vertical circle through the point.

REFERENCES

A-1. Schupler, B. R. and Clark T.A., "How Different Antennas Affect the GPS Observable," *GPS World*, Vol. 2, No. 10, Nov/Dec 1991, pp. 32-36.

A-2. Hermann, B., "GPS Antenna Phase Center Calibration," NSWCDD, Dahlgren, VA, 28 Oct 1992.

A-3. Corbin, T., "The Optical Reference Frame- Current Status, Existing Problems and Current Solutions," *Proceedings of the Annual DoD Applied Astrometry Forum*, 7-8 Mar 1995, U.S. Naval Observatory, Washington, DC, May 1995.

A-4. Kammeyer, P. C.; Fliegel H. F.; and Harrington, R. S., "Optical Astrometry and the Global Positioning System," *Proceedings of the 127th Colloquium of the International Astronomical Union, Reference Systems*, Virginia Beach, VA, Oct 1990, pp. 284-287.

A-5. Muellerschoen, R., et al., "Results of an Automated GPS Tracking System in Support of Topex/Poseidon and GPSMet," *ION GPS-95, 8th International Technical Meeting of the Satellite Division of the Institute of Navigation*, Palm Springs, CA, 12-15 Sep 1995, pp. 183-193.

A-6. Langley, R. B., *GPS.PRN27.CCD.GIF.UUENC.TXT*, CANSPACE File Archives, gopher://unbmvs1.csd.unb.ca., 1995.

DISTRIBUTION

	Copies
DOD ACTIVITIES (CONUS)	
ATTN D BREDTHAUER (ATPS MS D 85)	1
K CROISANT (ATIR MS 84)	1
S MALYS (ATIR MS D 84)	5
R SMITH (ATSS MS D 82)	1
DEFENSE MAPPING AGENCY ACQUISITION AND TECHNOLOGY GROUP 4600 SANGAMORE RD BETHESDA MD 20816	
ATTN J SLATER (OGC MS A12)	1
W STEIN (ATSS MS D82)	1
DEFENSE MAPPING AGENCY OPERATIONS GROUP 8613 LEE HIGHWAY FAIRFAX VA 22031-2137	
ATTN J WHITE (SMWD4)	3
DEFENSE MAPPING AGENCY OPERATIONS GROUP 1342 TULAROSA ROAD BLDG 841 HOLLOMAN AFB NM 88330	
ATTN R WIDEMAN (SMWD4)	1
DEFENSE MAPPING AGENCY OPERATIONS GROUP 15 N MUROC 4305 EDWARDS AFB CA 93524	
ATTN R STAKER (SMWD4)	1
DEFENSE MAPPING AGENCY OPERATIONS GROUP 1135 REDSTONE ROAD PATRICK AFB FL 32925	
ATTN CODE E29L (TECHNICAL LIBRARY)	1
COMMANDING OFFICER CSSDD NSWC 6703 W HIGHWAY 98 PANAMA CITY FL 32407-7001	

	Copies
DEFENSE TECHNICAL INFORMATION CTR 8725 JOHN J. KINGMAN RD SUITE 0944 FT BELVOIR VA 22060-6218	2
NON-DOD ACTIVITIES (CONUS)	
THE CNA CORPORATION PO BOX 16268 ALEXANDRIA VA 22302-0268	1
ATTN GIFT AND EXCHANGE DIV LIBRARY OF CONGRESS WASHINGTON DC 20540	4
INTERNAL	
E231	3
E282 (SWANSBURG)	1
K10	1
K104 (FELL)	1
K12	7
K12 (CUNNINGHAM)	12
K12 (HERMANN)	25
K13	1
K43 (MELKUN)	1
K43 (SITZMAN)	1